REPUBLIC OF IRAQ MINISTRY OF HIGHER EDUCATION AND SCIENTIFIC RESEARCH

AL-FURAT AL-AWSAT TECHNICAL UNIVERSITY

ENGINEERING TECHNICAL COLLEGE-NAJAF

CONVOLUTIONAL NEURAL NETWORKS BASED ON NON LINEAR FREQUENCY ESTIMATOR

RANA HASAN JAFAR MOHAMED

(B. Sc. In Communications Techniques Eng.)

2022

CONVOLUTIONAL NEURAL NETWORKS BASED ON NON LINEAR FREQUENCY ESTIMATOR

A THESIS

SUBMITTED TO THE (COMMUNICATION TECHNIQUES ENGINEERING DEPARTMENT)

IN PARTIAL FULFILLMENT OF THE REQUIREMENTS FOR THE DEGREE OF (MASTER)

BY

RANA HASAN JAFAR MOHAMED

Supervised by

Prof. Dr. AHMAD TAHA ABDULSADDA

2022

سورة االمجادلة/اية 11

Dedication

To the secret of my existence in life, to the one whose name I bear for Matt (my beloved father).

To the spring of tenderness that flooded me with her prayers and I had a candle that lit my path (my dear mother)

To My companion in my path, my life partner and my support (my beloved husband)

To my (dear daughters)

Declaration

I hereby declare that the work in this thesis my own except for quotations and summaries which have been duly acknowledged.

2022 Rana Hasan Jafar

Supervisor Certification

We certify that this thesis entitled " Convolutional Neural Networks Based on Nonlinear Frequency Estimator" which Rana Hasan Jafar is submitting was prepared under my supervision at the Communication Techniques Engineering Department, Engineering Technical College-Najaf, AL-Furat Al-Awsat Technical University, as a partial fulfillment of the requirements for the degree of Technical Master in Communication Engineering.

Signature:

Name: **Prof. Dr. Ahmad T. Abdulsadda**
(Supervisor)

Date: / / 2022

In view of the available recommendation, I forward this thesis for debate by the examining committee.

Signature:

Name: **Prof. Dr. Ahmad T. Abdulsadda**
(Head of comm. Tech. Eng. Dept.)

Date: / / 2022

Committee Report

We certify that we have read the thesis entitled "Convolutional Neural Networks Based on Nonlinear Frequency Estimator" submitted by Rana Hasan Jafar and as an Examining Committee, examined the student in its contents. Therefore in our opinion, it is adequate for the degree of Technical Master in Communication Engineering.

Signature:
Name: : **Dr. Ahmad T. Abdulsadda**
Degree: **Prof**
(Supervisor)
Date: / / 2022

Signature:
Name:**Dr. Husam Noman Mohammed Ali**
Degree: **Lecturer**
(Member)
Date: / / 2022

Signature:
Name: **Mohanad Hasan Ali**
Degree: **Asst.Prof**
(Member)
Date: / / 2022

Signature:
Name:**Dr. Musa H. Wali**
Degree: **Prof**
(Chairman)
Date: / / 2022

Approval of the Engineering Technical College- Najaf

Signature:

Name: **Assistant Prof. Dr. Hassanain G. Hameed**

Dean of Engineering Technical College- Najaf

Date: / / 2022

Language Expert Certification

This is to certify that this thesis entitled **"Convolutional Neural Networks Based on Nonlinear Frequency Estimator"** was reviewedlinguistically. Its language was amended to meet the style of the English language.

Signature:

Name: Asst. Prof. Raed Dakhil Kareem (PhD).

Date:

Abstract

One of the most recent problems is the frequency estimation in light of the distortion of the signal due to ambient noise, which makes it difficult to estimate its frequency. In this work, the problem has been dealt with in three cases of movement between the sender and the receiver. In the first case, the state of the sender and receiver is static. The mathematical model was designed using the Matlab program and estimates the frequency response of a linear system with a fixed time when the input is a sinstream signal. The correlation method is the algorithm used in this case. To work on the controller in the model where all kinds of controllers were used and we concluded that the best values of gain to get the best frequency estimation response are (5,500.2.5,.) kp, ki. Kd, respectively. After noise is applied to the system, we find that the best controller for the best estimate of the frequency response estimate is the PD controller when the gain values of Kp and Kd are 5 and 2.5, respectively.

In the second case, when the transmitter is stationary and the receiver is moving, such as the radar system and the target is moving at different speeds and accelerations, where the target is detected, and frequency estimation for it, the signal is processed using pulse compression techniques, observing the Doppler effect on the signal and estimating the frequency of the received signal in three cases of SNR (0db, 4db, and 8db) after converting it from a one-dimensional signal to a two-dimensional signal, and treating it as an image. The convolutional neural network algorithm was used, which is a non-linear estimator to estimate the frequency and get very good results with an accuracy of 99% in a natural environment, the target was detected and its frequency was estimated under complex conditions such as chaos background. The program has been re-simulated to get good results. The network has a proven efficiency and accuracy of 97%.

In the third case, the target was detected and the frequency was estimated when both the radar and the target were moving, the first was moving at a speed of 20 m/s, and the second was moving at a speed of 50 m/s and with an acceleration of 5 also, the convolutional neural network algorithm was used

Acknowledgments

I would like to thank Almighty God for granting me success in completing my scientific career and achieving my dream, and also all thanks, appreciation, and gratitude are to my supervisor, Professor Ahmed Taha Abdul-Saada, for the scientific support he provided me in my research career and for his valuable comments that raised the level of research. I am very proud to be part of his research team.

All thanks and appreciation are to my dear husband and companion in my path, who gave me the best support and assistance in my studies.

My sincere thanks are to my beloved father and dear mother for their love and support for me and my family during my studies.

My thanks are to all my brothers, friends, and everyone who supported me morally during my scientific career.

Without all the people mentioned above, I would not be the person I am today, all have given me the strength and drive to succeed and complete this project

Contents

List of Table page

List of figure

List of publications

[1] Rana Rasan Jafar, Ahmad Taha Abdulsadda "frequency estimation based on different techniques" published in the jornal of Global Sientific jornal(GSJ) which is scopuse indexed and has an impact factor. GSJ: Volume 10, Issue 6, June 2022, Online: ISSN 2320-9186

[2] Rana Rasan Jafar, Ahmad Taha Abdulsadda " Non-Linear Frequency Estimation by Non-Linear Estimator" published in the 1st international Conference Proceeding.the accepted manuscripts published in the API Conference Proceeding which is scopus indexed and has an impact factor. https://icasdg.atu.edu.iq/ojs/index.php/jounals

[3] Rana Rasan Jafar, Ahmad Taha Abdulsadda " Linear Frequency Estimation upone Convolutional Neural Network " Accepted in the Jornal of Robotics and controller. which is scopus indexed and has an impact factor. https://www.scimagojr.com/journalsearch.php?q=21101058819&tip=sid&clean=0

[4]] Rana Rasan Jafar, Ahmad Taha Abdulsadda " Non-Linear Frequency Estimation upone Convolutional Neural Network " Accepted in NAUN jornal. which is scopus indexed and has an impact factor. https://npublications.com/registrations.php

List of Abbreviations/ Nomenclature

Abbreviation	Definition
AC	Auto-Correlations
AFRC	Area's Frequency Response Characteristic
AWGN	Additive White Gaussian Noise
CFRFT	Continuous Fractional Fourier Transform
CNN	Convolutional Neural Network
CONV	Convolution Layer
CRB	Cramer-Rao Bound
CSL	Chinese Sign Language
DL	Deep Learning
EM	Electromagnetic Wave
EW	Electronic Warfare
FC	Fully Connected
FFT	Fast Fourier Transform
FRFT	Fractional Fourier Transform
FS	Fourier Series
FT	Fourier Transform
IF	Instantaneous Frequency
LFM	Linear Frequency Modulation
LFW	Labeled Faces in the Wild
LLS	linear Least-Squares Algorithm
LPI	Low Probability of Intercept
MIMO	Multi-Input and Multi-Output
ML	Maximum Likelihood
NLFM	Non-linear Frequency Modulation
NLS	Non-linear Least Squares
OFDM	Orthogonal Frequency Division Multiplexing Systems
PET	Pre-estimation Assisted Threshold
PID	A proportional-Integral-Derivative Controller
PTFT	Parameterized Time-Frequency Transform
RF	Radio Frequency

RWD	RadonWigner Distribution
SISO	Single Input and Single Output
SLCT	Simplified Linear Canonical Transform
SLR	Sign Language Recognition
SNR	Signal to Noise Ratio
STFT	Short Time Fourier Transform
WHT	Wigner-Hough transform

List of Symbols

Symbol	Description
σ_r	Cross sectional area
$R_\circ$	Distance between the target and the radar
T_n	Observation time
$v_\circ$	Initial velocity
A	Amplitude
B	Band width
C	Speed of light
D	Depth
Db	Decibel
F	Filed size
Fc	Carrier frequency
H	High
Kd	Derivative gain
Ki	Integral gain
Kp	Proportional gain
P	Padding
R_s	line-of-sight distance
S	Stride
t_m	Slow time
Tp	Pulse width
W	Wight
T	time delay
Φ	Phase
Ω	angular frequency
a	Acceleration
fd	Doppler frequency
g	jerk(acceleration change)
α	chirp rate for transmitter
λ	Wavelength

μ	Chirp rate for receiver
L_s	Simulink length
w_i	ith Frequency when the frequencies parameter in(rad/s)
$N_{freq,}$	Number of frequencies
$N_{set,i}$	Value of settling priod parameter
$N_{estim,i}$	Estimation period number
T_s	Sampling time of Simulink
$N(t)$	Noise
N	Number of sample

Chapter 2
Problem Formulation Theory

Chapter 1

Introduction and Literature Review

1.1 Introduction

In the past years, the problem of frequency estimation, as in Figure(1.1) which shows the multiple-tone radar system frequency method estimation, was present and it was addressed by researchers in different ways, including the old classics [1] using discrete Fourier transform (DFT) and using the s-transform [2] to obtain a frequency estimate. When there is noise, it can be removed by a subsequent step, which is the use of non-linear least squares (NLS) to remove noise from the signal and obtain a more accurate estimate despite its computational complexity. Solving the nonlinear functions yields the proposed estimator. [3] The new estimator has an analytical formulation based on three DFT samples and an interpolation approach to estimate the frequency of a complex exponential sine waveform observed under additive white Gaussian noise (AWGN). The suggested estimator has a lower SNR threshold than the Cramer-Rao estimator, demonstrating that its performance is near to that of the Cramer-Rao estimator bound (CRB) in the low-SNR, as well as its performance, in the high SNR area. In terms of its performance in the high SNR area, it beats earlier estimates. Because of the linear approach, the linear least-squares algorithm (LLS) should be used [4] to estimate the frequency of a single-tone noisy signal, which is more efficient than the nonlinear least-squares algorithm (NLS). This algorithm's methodology entails linearizing the frequency estimation problem by fitting a waveform with a similar but wrong frequency. Surprisingly, the right frequency can then be derived by doing so. When the signal frequency was known ahead of time within a 10% or greater range, excellent performance was achieved. The standard deviation of the estimator, for example, matched that of NLS when employing the batch version of the technique. Because LLS is non-recursive, it is substantially more computationally efficient than the recursive NLS. There are several methods used to estimate the frequency of a complex sinusoidal complex under white Gaussian noise, including the autocorrelation (Corr) method and the maximum likelihood (ML) method by fast Fourier transform (FFT). [5] The researcher used the automatic phase-correction method to estimate the frequency of the sinusoidal signal, and the method was good for reducing

the effect of the signal of non-half period sampling signal on autocorrelation. The second step is the generation of the reference signal using the phase correction autocorrelation signal. Finally, frequency estimation is performed by computing the minimum of an error function between the phase correction autocorrelation signal and the reference signal. The analysis of computing complexity, simulations, and experiments are done to show the superiority of the proposed method. [6]We notice that FFT is more efficient than (Corr), as the SNR of the correlation is (-15db) and the SNR of FFT is (-30db). That is, the difference between them is (15db). On the other hand, the approach of instantaneous frequency (IF) is one of the characteristics of the primitive wave shape can be found in many applications like communication, speech, and music processing. (IF) estimator [7] was estimated using the Winger distribution method based on the length of the window. The results were improved [8] by using an adaptive-short time Fourier transform, which provides the best rejection of co-channel interference. The S-transform technique was used in a white Gaussian noise environment [9], which was implemented through simulation, which showed that the bias and change depended on the signal.[10]The second-order statistics are reconstructed from compressed observations of a single sinusoid in MA colored noise for the purpose of frequency estimation of the original uncompressed noisy sinusoid using compressive covariance sensing. For moderate compression ratios, estimation accuracy is good, but it degrades for lower (better) compression ratios, resulting in a skewed estimate.

Due to the sensitivity of these applications, the detection and analysis of moving targets plays an important role in military and security applications such as monitoring security sites and determining the hobbies of aircraft. In this work, we used three cases to estimate the frequency, the first case, which is a basic case. A model was designed in the Matlab simulation program to find an estimate of the frequency response of the linear time invariant system by the aut-correlation algorithm. Also, work was done to add noise to the model using a block from the Matlab library, which is band-limitted white noise. As well as restarting the simulation and working to improve the results through the change in the control units and their gained value results are obtained.

In this thesis, we dealt with the solution to the problem of frequency estimation in three cases between the transmitter and the receiver; the first case is when both the transmitter and the receiver are stationary. In the second case, the radar system was worked on due to its importance in the military and security fields, where the target was moving at different speeds and

acceleration, and a set of data has been generated for this case of speed and acceleration. converting it into images for ease and accuracy of dealing with the convolutional neural network. The researcher used this technique [11] To categorize the 1.2 million high-resolution photos in the ImageNet LSVRC-2010 contest into the 1000 separate categories, we trained a huge, deep convolutional neural network(CNN). [12] One of the networks of this algorithm, Google Net, was used to discover and classify the radar signal with the Low Probability of Intercept (LPI), and it is considered one of the most important challenges in electronic warfare (EW), where nine types of radar modulation (LPI) were discovered and classified, including LFM, multi-phase, and multi-time

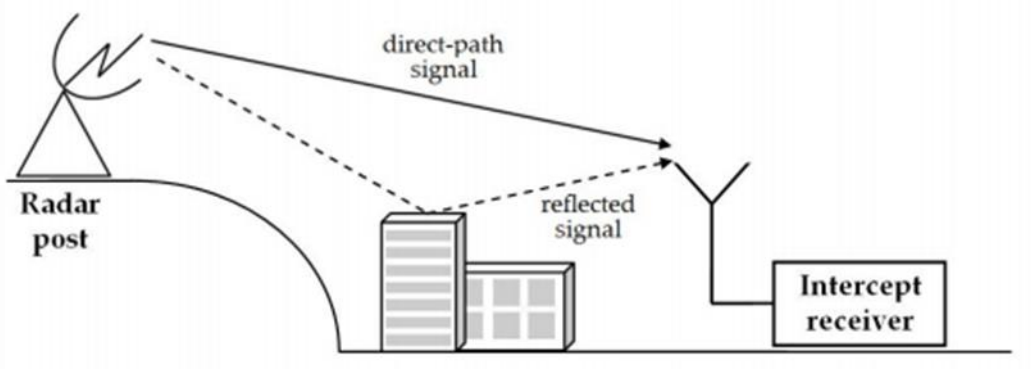

Figure (1.1) Multiple tone radar system estimation frequency method [13]**.**

1.2 Literature Review

In this chapter, the researcher aims to present the literature related to the topic of frequency estimation for fixed and mobile systems such as radar.

1.2.1 Frequency Response Estimation review

Per Dodin in 1996 [14]: it used spectrum estimation as a method to estimate the frequency

function response of a linear kinetic system by smoothing the frequency field using the window function. Both aircrafts were subjected to a technique for real-time estimation of frequency responses and their uncertainty.

Mao, Zhu Todd, Michael in 2013 [15] In this study, frequency response function (FRF) magnitude and phase H1-based estimations were statistically modeled using a Gaussian bivariate method, yielding analytical probability density functions (PDFs) of the estimates. Monte Carlo testing was used to evaluate the models using data from both simulation and real-world experiments. The magnitude and phase estimations' probability density functions (PDFs) are produced using a Gaussian bivariate statistical model. Both an ideal simulation test-bed and an experimental lab-scale structure are used to validate the suggested statistical model.The original data is contaminated with fake noise to further verify the resilience of the model. The histogram data and the projected PDFs line up quite well, which is why the outlier percentage is used in this study as a comparative metric. The outlier percentages constantly match the pre-described uncertainty thresholds for different degrees of significance, showing that the suggested statistical model appropriately estimates the uncertainty of FRF calculations using H1.

J. Grauer and E. Morelli in 2014 [16] **:** Data from flight tests and simulations are used. The method is recursively formulated and computationally straightforward enough to be real-time implementation very accurate when using the multi-sine inputs. A simple quotient can be used to create point estimates for the frequency responses. These point estimates can be combined to form an extremely precise frequency response estimation.

Polajžer, Boštjan, Dolinar, Drago, Ritonja, Jožef in 2015 [17]: The researchers worked on covering the methods for estimating the frequency response characteristic of the(AFRC) region during large frequency shifts. Since the previously available procedures had poor temporal accuracy and were highly distorted due to inaccuracy, the researchers suggested the technique of estimating the local correlation on the basis of the relationship between the frequency deviation and the change in the exchange capacity observed on all the connecting lines in the region. This technique was compared with the techniques used previously, such as least squares, which depend on the ratio of the average changes. The results indicated the accuracy and reliability.

Liu, Fushun Chen, Jiefeng Qin, Hongde in 2017 [18] **:** In their work, the researchers dealt with estimating the frequency response of the general structures by representing them with the retrieval function of the exponential complex. A frequency-domain response estimation technique for floating structures was put forth in this article. The issue of getting the Laplace domain expressions of additional mass and added damping was overcome by modeling the retardation functions with the Laplace domain expressions of the increased mass and added damping. Extensive and complex exponentials. The proposed method is not effective for estimating exciting wave forces in the frequency domain, confined to considering only harmonically composed forces, but when more components are included. They can produce accurate estimates. Because each part of these wave forces has a corresponding pole and residue in the Laplace domain, they were included in the original wave forces. The following conclusions are supported by numerical findings: (1) External excitations, such as wave forces, are not limited to harmonic ones and can have purely harmonic, damped harmonic, or solely damped exponential components. (2) The FRFs from the new methodology are very similar to those from the previous method. Particularly when these forces are actually made up of just harmonic components, the method can offer estimates of responses that are almost equal to those obtained using the conventional frequency-domain method.

Myronchuk, Oleksandr Shpylka, Oleksandr Zhuk, Serhii in 2020 [19]**:** In this research, a Kalman filter-based channel frequency response estimation approach for OFDM systems is proposed. The two-stage method only employs pilots from the current OFDM symbol. Pilot filtering is performed in the first step in both forward and reverse directions, with the results being combined at each point.in the second stage, the channel frequency response between the pilots is extrapolated in both the forward and backward directions, and the results are combined.
In this work, a simulation model was designed in Matlab to estimate the linear time-invaraint system frequency response using the automatic correlation algorithm and calculate the frequency response estimation in various control units and compare them with the frequency response estimation in the presence of noise in the system after adding it to the model to get the best estimate of the frequency response.

1.2.2 Linear Frequency Modulation estimation(LFM) review

Radar and modern communications systems are one of the most important fields that provide frequency estimation for a linear frequency modulation signal(LFM), and it is one of the most important unstable typical signals.

WANG JinZhen in 2014, [20]**:** The researcher used the noise SNR algorithm to estimate the parameters, including the frequency of the chirp signal, which was implemented in three steps: first, using a short-time Fourier transform to extract the frequency of the peaks of the chirp signal; secondly, using a suitable medium-sized filter to get rid of the defect frequencies and obtain the smoothing frequencies; and thirdly, constructing the frequency modulation line in a way to coarsen and remove the far points of frequency and, in this way, get less difficulty and more accuracy.

Mohsen Joneidi,2015 [21]**:** A quick and trustworthy approach for the estimation and detection of LFM signals is described. The implemented approach relies on concurrent sparse coding over two different dictionaries. Each dictionary has been specifically defined to look up a particular parameter. An iterative framework is also provided for the purpose of solving the concurrent sparse codes. The simulation results show that the proposed algorithm's accuracy is totally similar to that of the FRFT and WHT optimum transform algorithms. The suggested approach is also much more computationally efficient. As a result, it might be practical for real-time applications.

Qiang Chena, Yunjie Lib and Mengtao Zhu in 2017 [22] **:** The researchers implemented an algorithms based on The Short Time Fourier Transform (STFT) transformation for the purpose of obtaining accurate and fast estimation of parameters, including the frequency of LFM signal under high noise. A long window length in STFT was used to improve the signal.

Serbes, Ahmet in 2017 [23] : The researchers used computer simulation to propose an approximate analytical method for frequency estimation of a single- and/or multi-component signal from a linear frequency modulation signal in this paper. Utilizing computer simulations,

the effectiveness of the suggested LFM parameter estimate method is further demonstrated. Time-frequency, radar, and sonar signal processing are only a few of the LFM signal-related applications that the produced results may find.

Bai, Guo ;Cheng, Yufan;Tang, Wanbin;Li, Shaoqian in 2018 [24]**:** In this paper, the researchers have implemented the method of multi-discrete phase transformation and weight complementation because the methods that preceded. Despite their accuracy under the high signal-to-noise ratio, were difficult, expensive, and complex, but the algorithm that was used proved highly efficient in estimating, in addition to the lack of complexity**.**

Xingjian Dong, Shiqian Chen i**n 2018** [25] **:** A method was used to estimate the Doppler frequencies of radar signals, which is an excess Fourier model. In the first stage of the method, the chirping method was used to analyze the multi-component signals into some individual components, and then the parameterized time-frequency transform (PTFT) was designed with identical Fourier kernels to estimate the frequency of the new components. obtained and then used the common least squares method for the purpose of estimating the complex sides of the components.

Yong Guo, Lidong Yang in 2019 [26] **:** This research introduced a novel approach for the simplified linear canonical transform (SLCT)based parameter estimation of the LFM signal. Theoretical analysis and simulation are superior to (CFRFT) and (FRFT)-based techniques. Experiments show that the proposed method transforms the advantages of straightforward implementation, excellent accuracy, and independence from starting points. Additionally, the suggested parameters applied an estimating technique to quantify physical Newton's rings which are traditional optical signal properties. So, this increases the measurement's precision.

Xiaolong Chen in 2019[27]**:**A CNN-based approach to LFM signal detection and parameter estimation is suggested. The benefits of deep neural network feature learning are fully utilized. datasets of three different signal types, including signal chirp rate signal,LFM signal,and frequency signal.A variety of SNRs are constructed for training and testing.The (FT) and (FRFT) are replaced with trained CNNs.The results of simulations show that the recognition rate

increases when the SNR is larger.The three different signal types all have rates that are above 90%.

Zhang, Xuepan;Wang, Cheng;Yang, Chen;Zhang, Xuejing;Lin, Qingqing in 2019 [28] In this research, the researcher used the Radon-Wigner distribution(RWD) method of computing instead of searching, where the complexity of the calculations was reduced by reducing the O(MN) to O(2N). O(MN)mainly caused by the angles and ranges searching where M is the number of searched angle ,and N is the number of searched ranges, which made the method very efficient with less complexity.

Feng Xi, Member in 2020 [29] : This research takes into account a multiple input, multiple output (MIMO) radar that operates by sampling received radar echoes in one bit. The use of one-bit sampling greatly decreases the expense of the hardware, the amount of energy used, and the systematic complexity, but it also presents substantial difficulties in obtaining highly precise target information from one-bit quantized data. they propose a maximum likelihood (ML)-based technique that recovers a virtual array data matrix by iteratively maximizing the likelihood function and, from the recovered matrix, jointly predicts the angle and Doppler parameters. They can successfully utilize a computationally effective gradient descent approach to resolve the ML issue since it is convex. A pre-estimation assisted threshold (PET) strategy is created based on our analysis of the Cram'er-Rao bound (CRB) of the ML-based method.

In this thesis, the frequency was estimated in three cases. In the first case, the simulation system of the Linear Time Variant system was chosen to estimate the frequency response, where three types of control units were used and the best was chosen in the estimate. Also, the effect of band-limited white noise block was added to the system. It was found that the best estimate was at the control unit. PD controller. On the other hand, the values of the transmission function of the system were changed and an improvement was noticed in the frequency response estimation. In the second case, when the target was moving with the stability of the radar, the frequency was estimated under noise and clutter background, and the Doppler effect was observed from the product of the target’s speed and acceleration. The table (1.1) shows the summary of the results reached by researchers in previous studies.

1.2.3 Convolution Neural Network(CNN) review

With the development of the modern era, CNN has become important because of its more complex and learned structure compared to traditional machine learning methods [29]. The CNN trained by the deep learning algorithm has achieved important achievements in many applications, including image classification, signal processing, etc. The figure (1.2) shows the arrangement of the network within the artificial intelligence family.

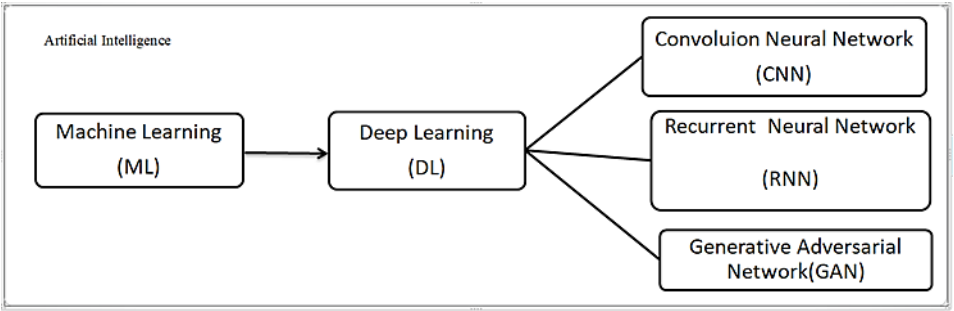

Figure (1.2). Family of Artificial Intelligence

Erdenebayar, Urtnasan;Kim, Hyeonggon Park, Jong-Uk;Kang, Dongwon;Lee, Kyoung-Joung in 2019 [30] : the authors presented a CNN model and improved it through normalization and dropout. The short-term normal ECG was examined using one-dimensional convolution, max-pooling, and fully-connected multiple perceptrons. To train and test the suggested CNN model, the ECG signal underwent pre-processing and segmentation. The two test sets and training sets were made up of MIT-BIH database contains an AF dataset and one normal dataset. The suggested CNN approach for the automatic prediction of AF performed well, with a sensitivity, specificity, and accuracy of 98.6%, 98.7%, and 98.7%, respectively. The outcomes demonstrate the potential for automatic AF prediction utilizing a short-term normal ECG signal and the CNN model. A useful tool for the early identification of AF in the medical field is the proposed CNN model for the automatic prediction of AF.

Abdeljaber, Osama; Sassi, Sadok;Avci, Onur;Kiranyaz, Serkan;Ibrahim, Abdelrahman Aly;Gabbouj, Moncef 1n 2018[31]: The study offers a quick, precise, and easy systematic method for ball bearing monitoring systems and severity detection online. This method makes use of tiny 1D, using convolutional neural networks (CNNs) to recognize, measure, and

pinpoints bearing damage. The suggested strategy is validated. A number of single and multiple damage experiments are used. The experiment's findings showed that the proposed method can get results with high precision for damage. detection, localisation, and measurement of damage The small and poorly trained 1D CNNs have real-time processing capabilities and greater robustness against high-level noise. The proposed strategy's core can manage fresh damage. with the highest degree of accuracy.

Bruno, Diego; Renan Osorio, Fernando S**antos in 2017** [32] **:** The researchers implemented a system to classify the images into different traffic signals such as stopping, maximum permissible speed, pedestrians, turning forward and slowing down using the convolutional neural network algorithm, and this aims to maintain the public safety on the road. It is considered an intelligent system that helps human drivers respect traffic rules and safety while driving the car. It has achieved good results with an accuracy of 97% of the test accuracy using reference data for known traffic signs (INI-Scale of the German Traffic Sign).

Ren, Shaoqing; He, Kaiming; Girshick, Ross; Sun, Jian in 2015 [33]: the researchers implemented the RPN region proposal network, which shares with the detection network the full convolutional features of the image, and this network is considered a fully convolutional network that predicts at the same time the degrees of the object at each position and its boundary. The fast R-CNN can be detected in a single network by sharing the features of the two convolutional networks to achieve the greatest speed and accuracy in object detection.

Schroff, Florian; Kalenichenko, Dmitry; Philbin, James in 2015 [34]

The author presented a Face Net is a system that immediately learns a mapping from facial images to a small subspace where distances are measured. A facial similarity metric can be directly equated to a Once Now where this area has been created. It is simple to implement activities like face verification, recognition, and clusters. Face Net is embedded as extracted features and conventional methods. A deep convolutional network was developed using our technique. The goal here is to directly improve the embedding itself instead of using a bottleneck layer in between like in earlier deep learning approaches. In order to train, we employ triplets of about generating matching or mismatching face patches with a new triplet mining online

technique. The advantages of our approach have significantly higher representational effectiveness. Utilizing state-of-the-art face recognition technology, a maximum of 128 bytes per face, this algorithm achieves a current record accuracy of 99.63% on its use of the wide Labeled Faces in the Wild (LFW) dataset.

Huang, Jie; Zhou, Wengang; Li, Houqiang; Li, Weiping in 2018 [35] : The author presented a 3D-Convolutional Neural Network (3D-CNN) for SLR that is attention-based. The structure offers two benefits: Convolutional 3D neural networks. Without prior knowledge, they discover spatial features from raw footage. To choose the hint, knowledge and attention mechanisms are helpful. 3D-CNN is trained to capture spatiotemporal characteristics. The network incorporates spatial attention to concentrate on the subject matters Following feature extraction, temporal focus is used to pick the important motions for categorization. The proposed approach is examined using two extensive sign language datasets. The first one is a Chinese sign that they have personally acquired 500 categories make up the Language (CSL) dataset. The CHALearn14 benchmark is an additional The experiment's findings. This shows how well their strategy works in comparison to cutting-edge algorithms.

Francisco Pastor, Juan M. Gandarias, Alfonso J. García-Cerezo andGómez-de-Gabriel, Jesús M.in 2019 [36]**:** the researchers presented the problem of identifying objects through active tactile perception using the 3D-CNN network by designing a robot grip that consists of two inactive fingers that adapt to the shape of different objects, and each of them has sensors used to touch and obtain its actual position. The network is designed to contain 24 elements, which they divided into three classes of materials: solid and changeable, which are in the bag; there are similar things and complex things like sponges; and the network has proven to work very well depending on the amount of well-trained large data

In this thesis, they have used the convolutional neural network in two-dimensional applications, first in detecting the target and estimating the frequency when it moves with different speeds and acceleration, and secondly, to classify the signals on the basis of speed and acceleration. The following table(1.1) summarizes CNN and results obtained by researchers in the former studies

Table (1.1) Summary of results reached by researchers in previous studies

Frequency response estimation			
NO	**Number of references**	**Approaches**	**Results**
1	[13]	spectrum estimation	estimate the frequency function response of a linear kinetic system by smoothing the frequency field using the window function. Both aircraft were subjected to a technique for real-time estimation of frequency responses and their uncertainty.
2	[14]	a Gaussian bivariate statistical model	This study tried that Both an ideal simulation test-bed and an experimental lab-scale structure are used to validate the suggested statistical model. The original data is contaminated with fake noise to further verify the resilience of the model. The histogram data and the projected PDFs line up quite well.showing that the suggested statistical model appropriately estimates the uncertainty of FRF calculations using H1.
3	[15]	Auto-correlation method algorithm	data from flight tests and simulations. The method is recursively formulated and computationally straightforward enough to be real-time implementation very accurate when using the multi-sine inputs. A simple quotient can be used to create point estimates for the frequency responses, and these point estimates can be combined to form a extremely precise frequency response estimation.
4	[16]	Local-correlation	worked on covering the methods for estimating the Area's frequency response characteristic (AFRC) during

			large frequency shifts, and since the previously available procedures had poor temporal accuracy and were highly distorted due to inaccuracy, The results indicated the accuracy and reliability.
5	[17]	A frequency-domain response estimation technique for floating structures	The following conclusions are supported by numerical findings: (1) External excitations, such as wave forces, are not limited to harmonic ones and can have purely harmonic, damped harmonic, or solely damped exponential components.(2) The FRFs from the new methodology are very similar to those from the previous method .Particularly when these forces are actually made up of just harmonic components, the method can offer estimates of responses that are almost equal to those obtained using the conventional frequency-domain method.
6	[18]	Kalman filter-based channel frequency response estimation approach	The two-stage method only employs pilots from the current OFDM symbol. Pilot filtering is performed in the first step in both forward and reverse directions, with the results being combined at each point. In the second stage, the channel frequency response between the pilots is extrapolated in both the forward and backward directions, and the results are combined.
Linear frequency modulation estimation			
7	[19]	the noise SNR algorithm	a short-time Fourier transform to extract the frequency of the peaks of the chirp signal; secondly, using a suitable medium-sized filter to get rid of the defect frequencies and obtain the smoothing frequencies; and thirdly, constructing the frequency modulation line in a way to coarsen and remove the far points of frequency.
8	[20]	sparse coding over two	The simulation results show that the proposed algorithm's

		different dictionaries	accuracy is totally similar to that of the FRFT and WHT optimum transform algorithms. The suggested approach is also much more computationally efficient. As a result, it might be practical for real-time applications.
9	[21]	Short Time Fourier Transform(STFT) transformation	of obtaining accurate and fast estimation of parameters, including the frequency of LFM signal under high noise. A long window length in stft was used to improve the signal.
10	[22]	Computer simulation to propose an approximate analytical	used computer simulation to propose an approximate analytical method for frequency estimation of a single- and/or multi-component signal from a linear frequency modulation signal, utilizing computer simulations, the effectiveness of the suggested LFM parameter estimate method is further demonstrated. Time-frequency, radar, and sonar signal processing are only a few of the LFM signal-related applications that the produced results may find.
11	[23]	multi-discrete phase transformation and weight complementation	because the methods that preceded it, despite their accuracy under the high signal-to-noise ratio, were difficult, expensive, and complex, but the algorithm that he used proved highly efficient in estimating, in addition to the lack of complexity**.**
12	[24]	Parameterized Time-Frequency Transform and Phase Compensation Technique	which is an excess Fourier model. In the first stage of the method, the chirping method was used to analyze the multi-component signals into some individual components, and then the parameterized time-frequency transform (PTFT) was designed with identical Fourier kernels to estimate the frequency of the new components. obtained and then used the common least squares method for the purpose of estimating the complex sides of the components.

13	[25]	Simplified linear canonical transform(SLCT)	The proposed method transforms the advantages of straightforward implementation, excellent accuracy, and independence from starting points. Additionally, the suggested parameters Application of an estimating technique to quantify physical Newton's rings are traditional optical signal properties, so This increases the measurement's precision.
14	[26]	Convolution neural network(CNN)	The (FT) and (FRFT) are replaced with trained CNNs. Simulation Results show that the recognition rate increases when the SNR is larger. The three different signal types all have rates that are above 90%.
15	[27]	Radon-Wigner distribution(RWD)	method of computing instead of searching, where the complexity of the calculations was reduced by reducing the O(MN) to O(2N). O(MN)mainly caused by the angles and ranges searching where M is the number of searched angle ,and N is the number of searched ranges, which made the method very efficient with less complexity.
16	[28]	Maximum Likelihood-based Method.	Efficient a multiple input, multiple output (MIMO) radar that operates by sampling received radar echoes in one bit. The use of one-bit sampling greatly decreases the expense of the hardware, the amount of energy used structure. SNR studies. Performance criteria.
Summary for CNN and result obtained by the researcher in former studies			
1`7	[29]	Time Series Prediction applications of 1-D	The suggested CNN approach for the automatic prediction of AF performed well, with a sensitivity, specificity, and accuracy of 98.6%, 98.7%, and 98.7%, respectively. The outcomes demonstrate the potential for automatic AF prediction utilizing a short-term normal ECG signal

			and the CNN model. A useful tool for the early identification of AF in the medical field is the proposed CNN model for the automatic prediction of AF.
18	[30]	Aplication of 1-D, signal identification	The experiment's findings showed that the proposed method can get results with high precision for damage. detection, localisation, and measurement of damage The small and poorly trained 1D CNNs have real-time processing capabilities and greater robustness against high-level noise. The proposed strategy's core can manage fresh damage. with the highest degree of accuracy.
19	[31]	Application of 2-D Image classification	It is considered an intelligent system that helps human drivers respect traffic rules and safety while driving the car. It has achieved good results with an accuracy of 97% of the test accuracy using reference data for known traffic signs (INI-Scale of the German Traffic Sign).
20	[32]	Application of 2-D Object detection	The fast R-CNN can detect in a single network by sharing the features of the two convolutional networks to achieve the greatest speed and accuracy in object detection.
21	[33]	Application of 2-D Face recognition	The algorithm achieves a current record accuracy of 99.63% on its use of the wide Labeled Faces in the Wild (LFW) dataset.
22	[34]	Application of 3-D Human action recognition	The CHALearn14 benchmark is an additional The experiment's findings. This shows how well our strategy works in comparison to cutting-edge algorithms.

23	[35]	Application of 3-D Object recognition/detection	the network has proven to work very well depending on the amount of well-trained large data

1.3 Problem Statement

Knowing the transmitter frequency when the noise level and the other harmonics frequencies appear rapidly in the signals generally speaking.This problem can be divided into:

- Choosing the system that has severed from this problem especially the radar system, drone communication system.
- Determining two cases fixed target and moving target.
- Non linearity of the transmitter signals will be considered.
- One solution is using deep learning technique such as (CNN).

1.4 Aim of the thesis

1. Designing and implementation nonlinear estimator CNN for the moving target system by :

- Deriving the mathematical modelling for the problem.
- Suggesting the nonlinear optimization techniques.
- Implementing it using the Simulink matlab program. The results would demonstrate the goodness of the suggestion methods.

2. Designing and implementation nonlinear estimator CNN for both radar and target are moving by:

- Deriving the mathematical modelling for the problem.
- Suggesting the nonlinear optimization techniques.
- Implementing it using the Simulink matlab program. The results would demonstrate the goodness of the suggestion methods.

1.5 Contributions

This work contributes to the frequency estimation in three cases of transmitting and receiving.

1. efficiency of estimating the frequency response when the transmitter and receiver are fixed by:
    - choosing the best gain values for the controllers, which is Kp(5),Ki(500) and Kd(2.5).
    - Introducing band limited white noise block into the system and estimating its frequency response with the best controller, which is PD controller.
    - A change in the values of the transfer function of the system and an improvement in the frequency response estimation were observed.
2. In the second case, when the sender is stationary and the target is moving using the radar system, the work has contributed to:
    - CNN techniques outperform traditional frequency estimation techniques in terms of efficiency.
    - converting the signal into an image and dealing with it in the network and observing the effect of each of the speed and acceleration, the so-called Doppler effect, on the estimation of the signal frequency.
    - Estimating the frequency under three cases, the signal-to-noise ratio(SNR) is 0db,4db,8db.
    - Frequency estimation under clutter background.
3. The third case is when both the target and the radar are moving, which is a new state for the detection of the target and the frequency estimation of it using the CNN algorithm .

1.6 Outline of thesis

Chapter 2: This chapter explains the problem formulation theory and mathematical model for three cases. It includes a theoretical introduction to the three cases of estimation, as well as a mathematical model for each case; an introduction to the algorithms we use in the work and their equations; and an explanation of the Doppler effect on the signal.

Chapter 3: This chapter explains the simulation model description and methodology. This chapter includes a description of the simulation of the system for frequency response estimation and the working algorithm and its detailed explanation, as well as an explanation of the algorithms used in the second case and how to process the signal. It also deals with the configuration of the data set used in the work in the form of images.

Chapter 4: This chapter includes the results obtained in the case of quantifying the frequency response, including the simulation results by changing the units of the count, as well as the results of changing the transfer function, as well as the results of programming from the second state to work from and output the convolutional neural network.

Chapter 5: This chapter includes the conclusions and future works, in addition to a table that summarizes the findings of the thesis.

1.7 Summary

The chapter dealt with an introductionto frequency estimation and survey of previous studies on frequency estimation and frequency response estimation, as well as adefinition of the CNN and its previous uses by researchers.

The research problem ,how to address it,aims and scientific contributions made by the thesis have been carified.

Chapter 2
Problem Formulation Theory

Chapter 2

Problem Formulation Theory

2.1 Introduction

The problem of frequency estimation existed in the past and it was dealt with in many classic ways, as we mentioned in the first chapter of this thesis. We have dealt with the solution to this problem in three cases:

- The first case is when both the sender and the receiver are fixed. A mathematical model was designed with the Matlab program and the linear time invariant system was selected.
- The second case is when the transmitter are fixed and the recipient is mobile, the radar system and the moving marine target have been selected, and the special algorithm was programmed. In this case, the CNN algorithm is programmed and processed with deep learning techniques.
- In the third, the same technique(CNN) is used to address the problem that preceded it in the second case, and compare them.

2.2 Frequency estimation

The theory of estimation is found in depth in many systems related to electronic signal processing, which are designed to extract parameters[37]. These systems include radar, sonar, speech, communication, control, and seismic science.

All of these systems share the problem of estimating a specific unit of measurement. For example, in this work,the radar system was selected due to the need to locate the target in this system to be used in important applications. So, the problem of estimating the range as well as

estimating the frequency became an essential task. A problem was worked on in this work. By estimating the frequency by knowing the speed of the target, it is possible to estimate the frequency received from the target. In this chapter, this problem has been dealt with different cases, and all the topics related to it were presented as shown by the scheme (2.1). We studied the traditional algorithms that researchers used previously and compared them with the algorithms used in this work.

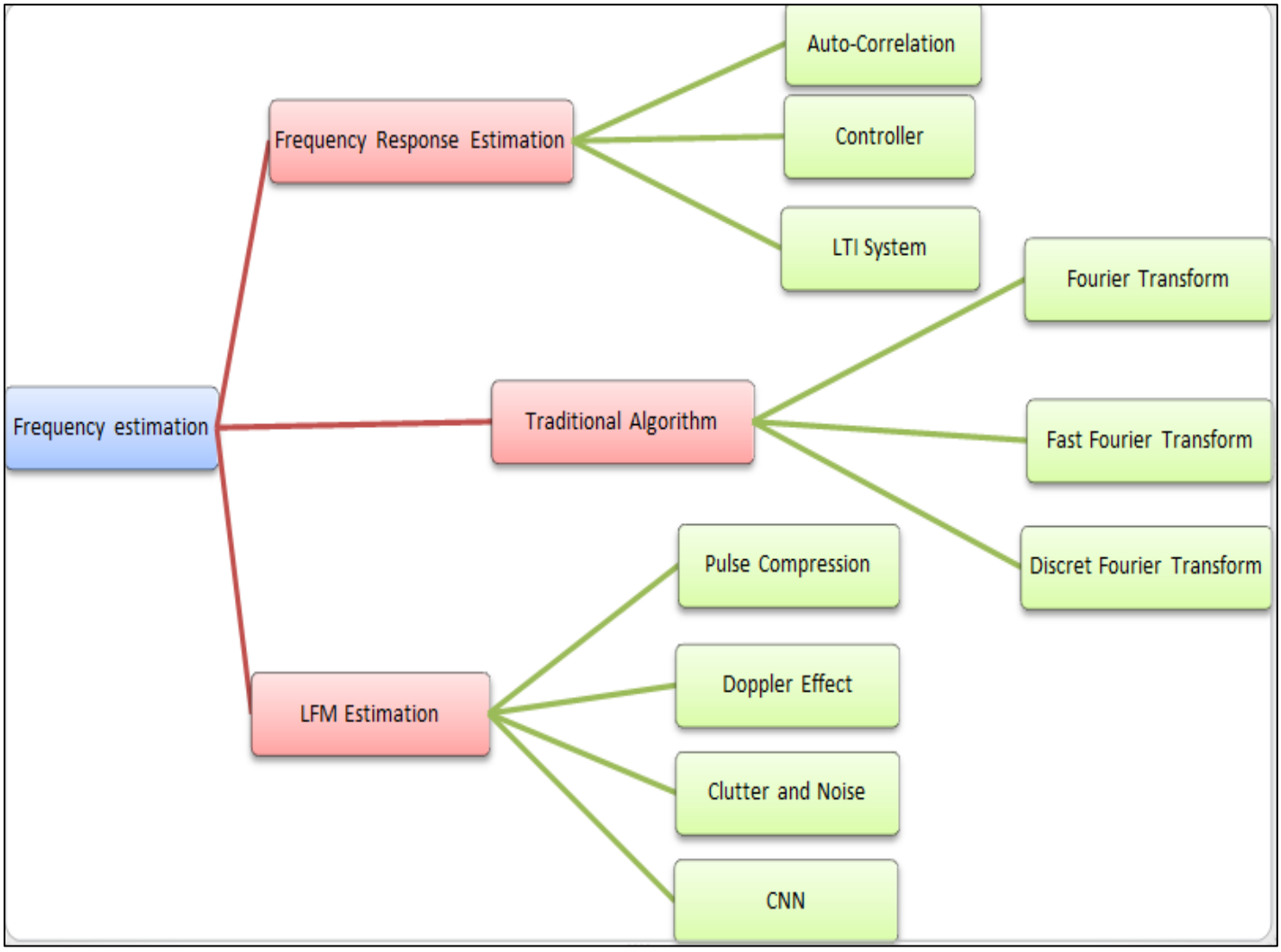

Figure (2.1) Block diagram showing the topics covered in Chapter Two

2.2.1 Fourier Transform (FT)

Periodic signals with period ($T_\circ$)and fundamental frequency $F_\circ = \frac{1}{T_\circ}$ can have their frequency content revealed using the Fourier Series (FS). We can make $T_\circ$ infinite to evaluate

nonperiodic signals. This limit transforms FS into the Fourier transform (FT). A Fourier transform pair refers to the relationship between a time-domain signal and its corresponding Fourier Transform; the signal or (FT) can be generated using (FT) and its inverse version as shown below.

$$X(f) = \int_{-\infty}^{\infty} x(t) e^{-2\pi j f t}\, dt \quad [38] \quad (2.1)$$

Inverse Fourier transform

$$x(t) = \int_{-\infty}^{\infty} X(f) e^{2\pi j f t} df \quad (2.2)$$

Let $x(t)$ the input signal , f the frequency , t the time

The Fourier transform, commonly known as the signal spectrum, is typically employed to expose the frequency information—also known as the content—of any signal, whether it be periodic or not. For periodic signals, such as sinusoids, a train of delta functions in the frequency domain, located at the fundamental frequency and its harmonics, can be constructed for all elements of its FS (which are complex sinusoids). The frequency response, also known as the transfer function of the system in system analysis, is obtained by applying Fourier transform to the system impulse response. It equals the system output divided by the system input, both in frequency domain, i.e., the output spectrum divided by the input spectrum (pointwise). It also uses the Fourier transform to process the radar signal[39].

2.2.2 Discrete Fourier Transform

Fourier Transform of analog signals (natural signals like speech) has infinite points, hence, it cannot be processed using digital systems. Hence, we should sample the signal and its spectrum. There would be no loss of information if the time-domain signal is sampled at NY Quist rate, which is twice the signal bandwidth (the bandwidth BW is the maximum frequency that is present in the signal spectrum). Similarly, it has been sampled the sampled FT which is called DTFT, uniformly as is the case in the time-domain, but the spacing between frequency samples is now $\boldsymbol{F_s}$ (in time-domain it was $\boldsymbol{T_s}$). we need this frequency-domain sampling to keep information. If selected the sampling rate in the frequency domain as $\boldsymbol{F_s = f_s/N}$, which forces the fact that the number of samples in the frequency domain equals those in the time domain, then this choice will ensure that there is no information loss. This sampling leads to discrete FT (DFT) as follows.

$X_s(k) = \sum_{n=0}^{N-1} X_s(n) e^{-\frac{j2\pi kn}{N}}$ $K = 0,1,2, \ldots N-1$ [40] (2.3)

To get back the time-domain signal, the inverse of the DFT $\boldsymbol{X_s(k)}$ is used as follow

$X_p(n) = \frac{1}{N} \sum_{K=-\infty}^{\infty} X_s(k) e^{\frac{j2\pi kn}{N}}$

$X_s(K) = \sum_{n=0}^{N-1} X_p(n) e^{-j2\pi kn/N}$ (2.4)

The idea behind sampling the DTFT is that the process of sampling in any domain causes content-replication (and scaling) in the other domain. If we follow NY Quist conditions, then no information is lost, otherwise aliasing occurs. Hence, the DFT is obtained from the DTFT via sampling the frequency content of DTFT at a sampling rate of $Fs = fs/N$. At this frequency-sampling rate, we can keep equal numbers of samples in both domains (which is N=time-domain samples). Now we have two transforms which are finite as follows (DFT and inverse DFT (IDFT).

$X(n) = \frac{1}{N} \sum_{k=0}^{N-1} X(k) e^{j2\pi kn/N}$

$X_s(k) = \sum_{n=0}^{N-1} X(n) e^{-j2\pi\pi kn/N}$ (2.5)

IDFT={DFT[X(n)]}=1 (2.6)

That is, the DFT and IDFT are reversible discrete and finite transforms, suitable for discrete signal representation and both having the same amount of samples [41].

2.2.3 Fast Fourier Transform(FFT)

It is a fast algorithm that is used to calculate the discrete Fourier transform (DFT) or its inverse (IDFT)in a faster way, because the discrete Fourier transform needs a long time when dealing with long signals. When the input signal samples are large, it requires a lot of time to perform the DFT process directly, especially in high-resolution signals. They have many samples, so they use FFT. They need the signal samples to be raised to the power of 2. In this work, the Matlab (fft) function was used. This algorithm has been used in pulse compression operations to process the received signal from the target.

2.3 Frequency response estimator

Frequency response is a description of the steady-state response of the system to the frequency-varying sinusoidal input as shown in figure (2.2), which allows us to analyze and

design control systems in this field. When we have a linear system in the modulation of the transmission function, as in the one used in this work, it is a linear-time invariant system(LTI) . Then there are three ways to plot the frequency response.

- Bod plot
- NY Quist plot
- Nichol chart

In this thesis, it has been used the bod plot to plot the frequency response of the system.

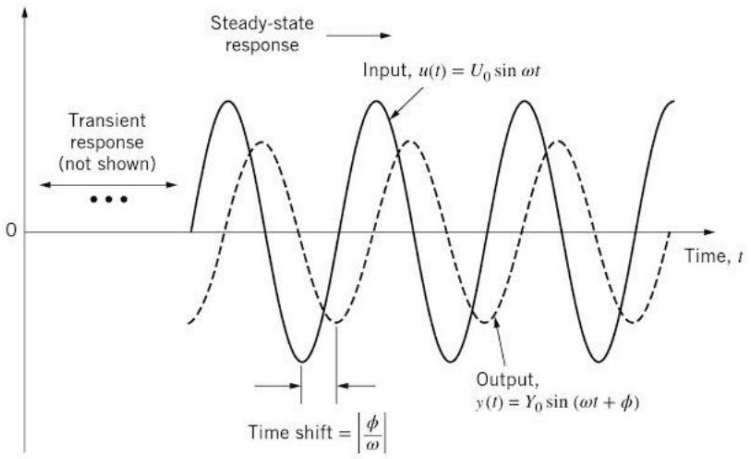

Figure (2.2)input and output sinusoidal functions[42]

To carry out model-based estimating in real time with a physical plant or in a Simulink model during simulation,The Frequency Response Estimator block has been used. To estimate the frequency response, the block concurrently does the following:

- injects sinusoidal signals at the plant's nominal operating position.
- gathers reaction information from plant output.
- The predicted frequency response is calculated.

In order to monitor system response, you specify the frequencies at which you disturb the plant. Through a start/stop signal, the estimating process is started. This signal enables you to begin estimating at any time, usually when the plant is functioning at its nominal point. As soon as the frequency responses converge, you halt the estimation. Any stable SISO plant can use online frequency response estimation. An unstable plant should be online. In this block, there are two options for input; either it is a Sine stream mod and has an autocorrelation (AC) algorithm for the

estimate, or it is a superposition and it has a RLS algorithm.

2.3.1 Sine stream mode

For frequency response estimation, use the Sine stream object to represent a sine stream input signal. A signal like this is made up of sine waves of varied frequencies that are applied one after the other. For a short amount of time, each frequency excites the system. As figure (2.3)

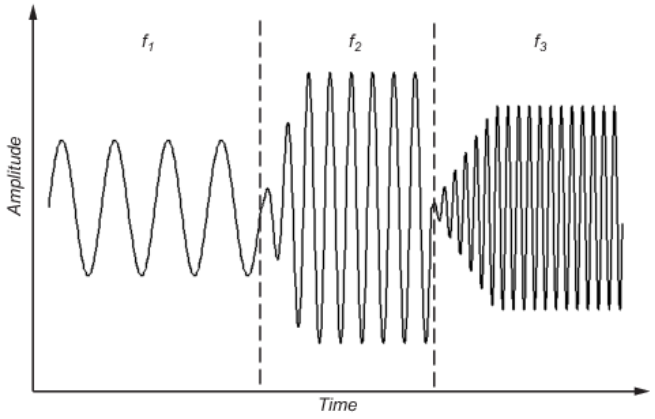

Figure(2.3)sinestream signal[43]

The signal enters at a certain frequency to the control (PID)and is transmitted to the system and then the output from the system is back-fed to the PID control and is compared with the other input signal whose frequency varies and the result of the comparison is generated an error that enters the estimation block and the estimation process begins by means of the correlation analysis algorithm and thus the sine stream signal continues to enter one by one, with different frequencies.

2.3.2 Correlation method algorithm

It is also known as the series correlation in the case of discrete time, and it is known as the link of the signal with a copy of the same signal, but with a delay. Another interpretation of it is a mathematical function used to find patterns that are repeated and disappear due to the effect of confusion, and this process is widely found in signal processors for function analysis

In this work, the correlation method analyzer works as figure (2.4) the measured system output is multiplied by both the sine and cosine of the input signal frequency(w), and then the output of the multiplication operations is entered into two identical integrals. The mean time T increases

its contribution to the regression of the unwanted frequency components to zero and that both the outputs of the integrals R(T) and I(T) become constant values that depend on the gain and phase in the transfer function of the system

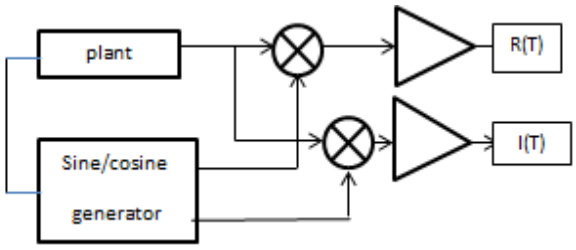

Figure (2.4)correlation block diagram

the mathematical model of this algorithm is:[44]

$$U(t) = A\sin(\omega t) \tag{2.7}$$

Where (A)is amplitude and(ω) is angular frequency

$$Y(t) = Y\sin(\omega t + \Phi) \tag{2.8}$$

Where $Y = U\,|G(j\omega)|$ and $\Phi = \angle G(j\omega)$

$$R(T) = \frac{U}{T}|G(j\omega)| \int_0^T \sin(\omega t)\sin(\omega t + \Phi)dt \tag{2.9}$$

$$= \frac{U}{T}|G(j\omega)|\{\cos\Phi\left[\frac{T}{2} + \frac{\sin 2\omega t}{4\omega}\right] - \sin\Phi[\frac{\cos 2\omega t}{4\omega} - \frac{1}{4\omega}] \tag{2.10}$$

When $T = \frac{N\pi}{\omega}$, N=1,2,3.....

$$R(\frac{N\pi}{\omega}) = \frac{U}{2}|G(j\omega)|\cos\Phi \tag{2.11}$$

$$I(T) = \frac{U}{T}|G(j\omega| \int_0^T \cos(\omega t)\sin(\omega t + \Phi)\,dt \tag{2.12}$$

$$I(\frac{NT}{\omega}) = \frac{U}{2}|G(j\omega)|\sin\Phi \tag{2.13}$$

$$\text{Fest} = \frac{\text{FFT Y(T)}}{\text{FFT U(T)}} \tag{2.14}$$

Fest is frequency estimation

2.3.3 Plant (linear-time invariant system)

In this part, the system used in the work is the linear time invariant system, which is a dynamic system where the stability state of (zeros, poles and gain) or transfer function can be determined. The transfer function (tf) is(10[1 10 1000]) This part was also dealt with and

changed in finding the best cases for estimating the frequency response by changing the transmission function of the system.as explained in the result chapter (4.2.3)

$$G(z)= \frac{10}{z^2+10z+1000} \quad (2.15)$$

2.3.4 Controller

Controller it is the feedback control mechanism, which is widely used in industrial control systems and is considered an inverse control mechanism in the control loop. It is used to measure the error ratio between the measured process and the desired set point.

There are five type of control unit (PID, PD, PI, P and I) controller The control unit (PID) has three separate and constant declarants. The three-term control unit is called the proportional, integral, and derivative values. These values can be interpreted in terms of time;

- (P) depends on the present time
- (I) depends on the accumulation of past errors
- (D) predicts future errors

In this work, the controller block in figure (2.5) was used to represent parallel discrete - time domain. The formula of each part of the controller[45].The term of the integral can be represented in discrete-time domain is :

Backward Euler $\frac{K_i T_S Z}{Z-1}$ (2.16)

Forward Euler $\frac{K_i T_S}{Z-1}$ (2.17)

Trapezoidal Euler $\frac{K_i T_S}{2}\frac{Z+1}{Z-1}$ (2.18)

Where K_i is the integral gain , T_s is sampling period

The term of derivative can be represented in discrete-time domain is

Backward Euler $\frac{N(Z-1)}{(1+NT_S)Z-1}$ (2.19)

Forward Euler $\frac{N}{1+NT_S Z/(Z-1)}$ (2.20)

Where N is derivative filter cofficient , T_s is sampling period

Trapezoidal Euler $\frac{N}{1+NT_S(Z+1)/2(Z-1)}$ (2.21)

In this model used Backward Euler of integration term and Forward Euler in drivative term in PID controller

$$C(Z)=K_p+\frac{K_i T_s Z}{Z-1}+\frac{K_d N}{1+NT_s Z/(Z-1)} \quad (2.22)$$

where $K_p$is proportional gain ,K_d is derivative gain, K_i is integration gain,N is derivative filter cofficient and T_s is sampling period

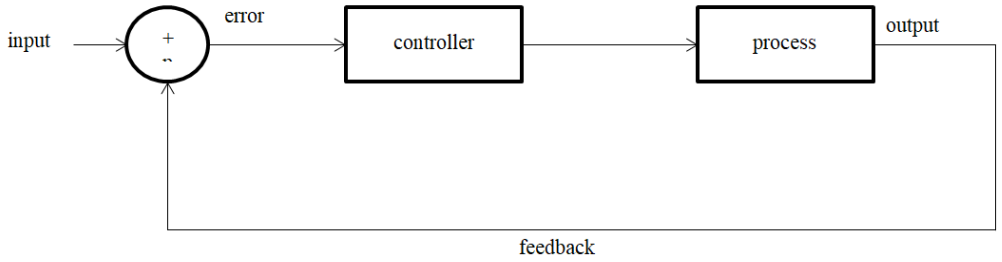

Figure (2.5) PID controller

2.4 Linear Frequency Modulation(LFM)estimation

The Linear Frequency Modulation (LFM) signal is a non-stationary signal that is used in radar and communication systems. For radar electronic reconnaissance and resistance, it is critical to quickly recognize and estimate the parameters of LFM signals. we used the radar system as an example to detect a moving target and estimate its frequency, and that the moving target of the radar is an important and sensitive topic in civil and military applications as it is closely related to the signal movement, and the enemy movement is linked to changing the speed of the target. In this thesis, it has been considered that both the target and the radar are in the same horizontal plane. In linear frequency modulation, the frequency increases or decreases linearly during the duration of the signal pulse. When the frequency increases linearly, it is called the up-chirp rate, and if the frequency decreases linearly, it is called the down chirp rate, as shown in the figure (2.6)

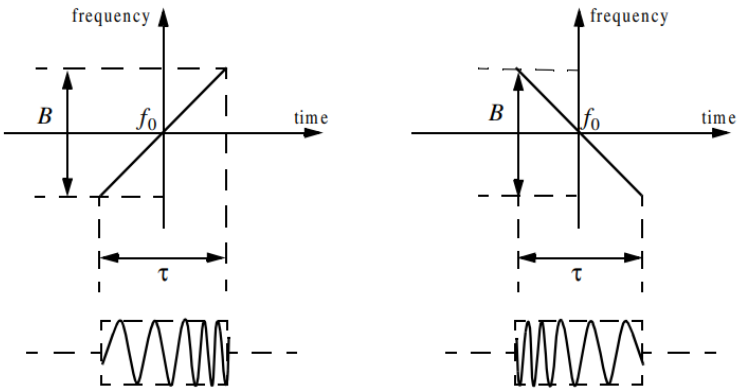

(a) (b)

Figure(2.6) Typical linear wave form (a)up-chirp (b)down-chirp[46]

Increasing the duration of the transmitted pulse increases its energy and ability to detect the target, while decreasing the duration of the pulse increases the radar range's accuracy.The radar transmits an LFM signal.

$S_t(t)=\text{rect}(\frac{t}{tp})\exp\{2\pi j[f_c t+\frac{1}{2}\alpha t^2]\}$ (2.23)

Where $\text{rect}(u)=\begin{cases}1, & |u|\le\frac{1}{2}\\ 0, & |u|>\frac{1}{2}\end{cases}$,f_c is the carrier frequency of radar, tp is the pulse width , $\alpha=\frac{B}{tp}$ is the transmitted signal's chirp rate, B is the bandwidth

The recived echo signal at time t is:

$S_r(t)=\sigma_r\text{rect}(\frac{t-\tau}{tp})\exp\{2\pi j(f_c[t-\tau]+\frac{1}{2}\alpha[t-\tau]^2)\}$ (2.24)

Where σ_r is the cross − sectional area of the target ,

$\tau=2\pi R_s(t_m)/c$ (2.25)

where c is the speed of light and τ is the time delay , The radar's line-of-sight distance from the target is R_s , and the slow time between the pulse and the pulse is t_m.

2.4.1 Cross -sectional area(σ_r)

It is the amount of power spread from the target towards the radar, and usually the electromagnetic waves are scattered in all directions when they fall on a specific target [47]. These scattered waves are categorized into two parts.

- It consists of waves having the same polarization as the receiver and is called the principle polarization(PP)
- It consists of waves that have a polarization different from that of the receiver, and it is called orthogonal polarization(OP)

2.4.2 Pulse compression

Pulse compression techniques[47] are very important to improve the accuracy of the radar range, as the accuracy of the radar range can be increased by using very short pulses. This may lead to a decrease in the average transmitted power, which in turn affects the normal radar operations, especially in multifunctional and monitored radars. Therefore, pulse compression techniques were used that allow us to achieve the average transmitted power of a long pulse at the same time, obtaining the accuracy of the short pulse range. There are two types of pulse compression techniques: correlation and stretch processing. The first type is used in this thesis, which is achieved by adopting the following steps:

[48]-[49] by following steps:

A. Applying the Fourier transform to the echoes that were received.

$$S_r(f) = \sigma_r \int_{-\infty}^{\infty} rec(\frac{t-\tau}{t_p}) e^{\{2\pi j(fc[t-\tau]+\frac{1}{2}\alpha[t-\tau]^2)\}} * e^{-j2\pi f_c t}\, dt \quad (2.26)$$

B. Taking the transmitted signal's complex conjugate (reference signal)

$$S_{tc}(t) = rec(\frac{t}{t_p}) e^{-j2\pi(f_c t+\frac{1}{2}\propto t^2)} \quad (2.27)$$

C. Performing the Fourier transform on the complex conjugated signal mentioned above.

$$S_{tc}(f) = \int_{-\infty}^{\infty} rec(\frac{t}{t_p}) e^{-j2\pi(f_c t+\frac{1}{2}\propto t^2)} * e^{-j2\pi f_c t}\, dt \quad (2.28)$$

$where\ S_{tc}$ is complex conjugated of transmitted signal

D. Multiplication of the two FFT signals we get

$$S_{pc}(f) = \sigma_r rect(\frac{t-\tau}{t_p}) sinc[t_p(\alpha\tau + f)] e^{-j2\pi f_c \tau} \quad (2.29)$$

E. Taking the IFFT of the above

We get

$$S_{pc}(t,t_m) = A_r sinc(B[t-\tau]) exp(-2\pi j f_c \tau) \quad (2.30)$$

Because of the radar movement at different speeds, the distance between the target and the radar

can be expressed in the Taylor series.

$$Rs(t_m)=R_\circ - vt_\mathrm{m} - \frac{1}{2!}\acute{v}t_m^2 - \frac{1}{3!}v^{'}\ldots,\ t_\mathrm{m}\in\left[-\frac{T_n}{2},\frac{T_n}{2}\right] \quad (2.31)$$

where v is the radial velocity of the target,and T_n is the observation time. Only the first four terms from the above equation are used as an approximation of the observation distance, so the equation has been reformulated as follows:

$$Rs(t_m)=R_\circ - v_\circ t_\mathrm{m} - \frac{1}{2}at_m^2 - \frac{1}{6}gt_m^3 \quad (2.32)$$

where $R_\circ$ is the distance between the target and the radar, $v_\circ$ is the initial velocity, a is the acceleration , g is the jerk(acceleration change).

2.4.3 Doppler effect by moving target

The Doppler Effect is the perceived shift in frequency or pitch that occurs when a sound source travels either toward the listener or away from the listener or when the listener moves either toward or away from the sound source. All wave motion is subject to this principle, which was discovered by the Austrian physicist Christian Doppler.[50] The apparent frequency difference between a wave's source and receiver is caused by the relative velocity of the source and the receiver. Assume that the source's sound frequency is constant in order to comprehend the Doppler Effect. Additionally, the sound's wavelength won't change. The receiver will hear the same frequency sound generated by the source if the source and the receiver of the sound are both stationary. This is due to the fact that the source and receiver both produce an equal number of waves every second. The receiver will now hear a higher frequency sound if either the source or the receiver, or both, move toward the other. This is due to the fact that the receiver will pick up more sound waves per second and perceive the extra waves as higher frequency sounds. In contrast, the receiver will hear fewer sound waves per second and a lower frequency of sound if the source and the receiver are moving apart. The frequency of the sound generated by the source will have stayed the same in both scenarios.

The radar[51] sends an electromagnetic signal and receives a reflected signal that has a time delay. The radar can measure the target’s range. If the target is moving, the frequency of the received signal will be shifted from the frequency of the received signal, known as the Doppler effect[52]-[53] and the Doppler frequency shift is determined by the radial velocity of the moving target[54] as equation below

$$f_t = \frac{c \pm v_t}{c \pm v_r} f_r \quad (2.33)$$

Where f_t is transmitter carrier frequency , f_r is received frequency

c is speed of light , v_t is velocity of target , v_r is velocity of radar

in the second case ,the radar is fixed and the target is moving ($v_r = 0$) ,and

$$f_d = f_t - f_r \quad (2.34)$$

Where f_d is doppler frequency substitute in eq(2.32) we obtain

$$fd = \frac{2v_t}{\lambda} cos\theta \quad (2.35)$$

In fact, the quantity of Doppler frequency depends on the component of the target velocity in the direction of the radar radial velocity and that the angle θ is considered the total angle between the line of sight of the radar and target, where λ is the wavelength

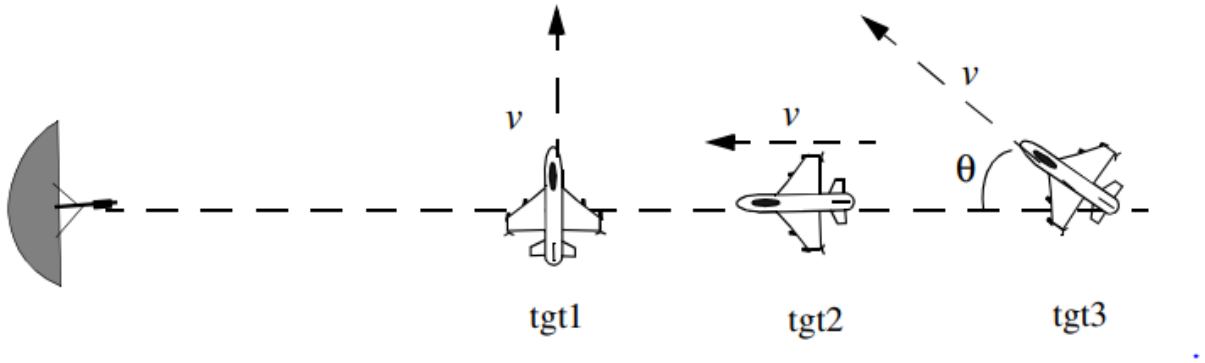

Figure (2.7) Angle positions between the target and radar velocity

Figure (2.7) shows the value of the Doppler frequency according to the direction of the speed of the target in relation to the radar. This work represents the second target(tgt2) in the figure, as the angle between the target and the radar is zero because the target is in the direction of the radar, so the Doppler frequency is maximum.The uniform motion has been dealt with, acceleration and Doppler spectrum for uniform motion displacement as in Equation (2.36), acceleration change for Doppler spectrum as in Equation (2.37)

$$fd_1 = 2v_t/\lambda \quad (2.36)$$

$$fd_2 = 2(v_t + at_m)/\lambda \quad (2.37)$$

$$f_\circ = 2vt/\lambda \quad (2.38)$$

$$\mu = 2a/\lambda \quad (2.39)$$

Equations (2.38) and (2.39) show the relationship between initial frequency $f_\circ$ and chirp rate μ

with target velocity $v_t$and acceleration a ,mathmatical model signal of radar recived from moving target as shown in eq (2.39) below:

$$S(t_m) = A_\circ \exp[j(2\pi f_\circ t_m + \pi\mu t_m^2)] \quad (2.40)$$

These Doppler shifts can be leveraged to the benefit of radar to identify echoes from moving targets in the presence of considerably louder echoes from stationary clutter or to significantly increase cross-range resolution.

As for the third case, which is when both the radar and the target are moving, but the movement of the radar is less compared to the movement of the target. And that the Doppler effect is on both the target and the radar as figure shown in (2.8), but without accelerating the radar. The equation (2.24) can be reformulated according to the third case

$$f_\circ = \frac{2(v_t+v_r)}{\lambda} \quad (2.41)$$

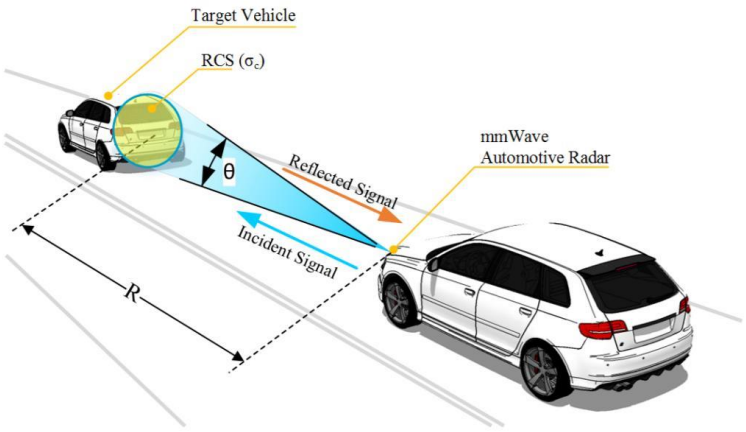

Figure (2.8) both radar and target is movement[52]

2.4.4 Clutter and Noise

The noise in the radar receivers is white Gaussian noise (WGN), which reduces the radar's ability to detect a target.in this thesis three value of SNR (0db,4db,8db) have been used to the moving target is detected and the frequency is estimated in the case of its movement at different speeds and rotation and in the presence of WGN. We also note the change in the shape of the received signal, as shown in Chapter Four. We also chose more difficult environmental conditions, which is the presence of clutter,[55] which means all the undesirable echoes signals in electronic systems, especially in the radar system, where there are signals from rain, trees,

meteor and buildings ,etc., and other signals received by the radar, which can be a major reason for reducing the efficiency of the radar at work, and the figure (2.9)show types of clutter:

- **Surface** Clutter Surface clutter is typically caused by ground or ocean returns[56] Although returns from geographical land masses are typically immobile, the target may impart a Doppler shift to the radar return due to the effect of wind on trees and other objects. This Doppler shift is a crucial technique for eliminating unwanted signals in the radar system's signal processing section. The movement of the waves is typically present in debris that has been retrieved from the sea.
- **Volume Clutter** Volume clutter is frequently weather or chaff. The most serious issue in the air is weather clutter. This can be made from snow or rain and can contain a lot of Doppler energy**.**
- **Point Clutter** Birds, windmills, and single towering buildings are examples of point clutter and do not occur naturally. Sometimes moving point clutter is referred to as "angels." Due to the similarities between their properties and those of airplanes, the clutter produced by birds and insects can be exceedingly challenging to eliminate.

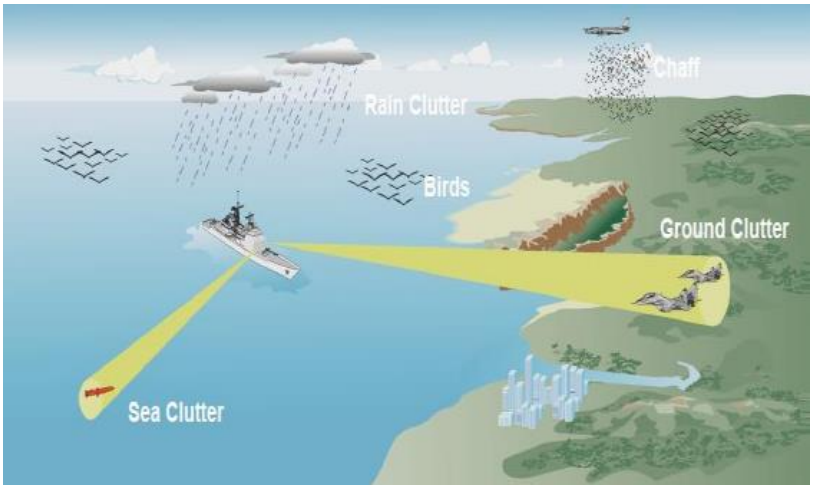

Figure (2.9) type of clutter[57]

2.5 Convolution Neural Network(CNN)

Over the past decade, deep learning technology has made important achievements in many areas of research,[58] such as radar signal processing, speech and voice recognition, so the radar data was applied as input to various deep learning algorithms, such as the convolutional neural network algorithm used in this research, which achieved success in terms of the use of large data, in addition to high accuracy, is not in the results. It is called a "deep neural network" because it consists of several layers, and it is also called a "convolutional neural network" because of the linear arithmetic process between matrices is called convolution. [59]

This algorithm has been used to classify images and extract features in this work. The dataset used depends on the speed and acceleration of the signal to detect the target signal and estimate its parameters into a two-dimensional

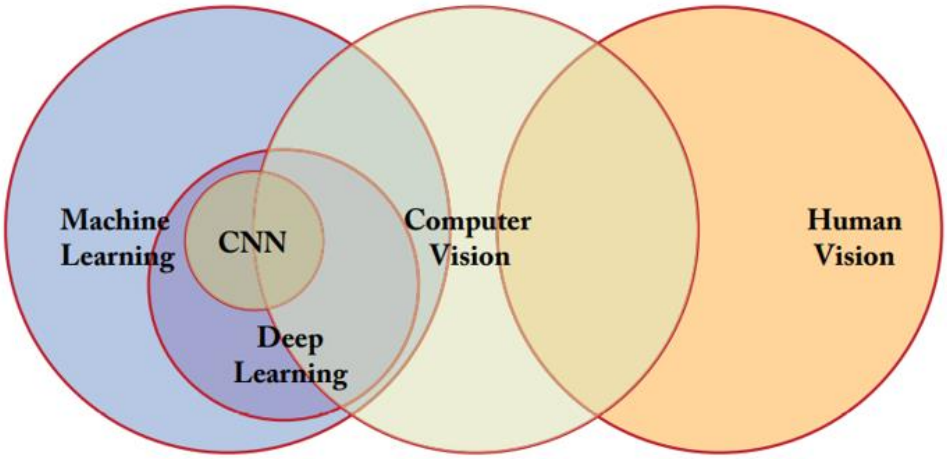

Figure (2.10) relationship between human vision and computer vision and machine learning[60]

The three-dimensional convolutional neural network inputs are height, width, and depth, as shown in Figure (2.11)

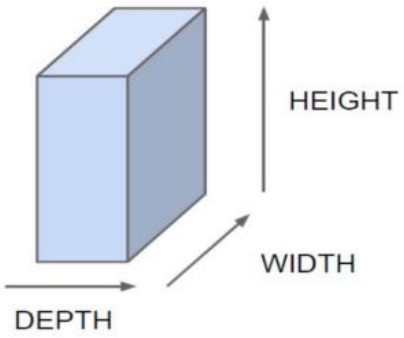

Figure (2.11) representation of three-dimension input of CNN[60]

In order to have good knowledge of the convolutional neural network, we must know its basic components, which consist[59]of:

2.5.1. Convolution layer(CONV)

This layer is very important in extracting features, which consist of several convolutional units. The purpose of this layer is to perform the convolution operation that will extract the low-level features[61]. Increasing the convolutional layers increases the accuracy of extracting more complex features, and the convolution process is done through dot multiplication between two matrices. One of them is called the kernel matrix, which is much smaller than the input matrix, but much deeper. Figure (2.12) explains the convolution process. The following three factors can be used to regulate the output size:

- **Depth**: The quantity of neurons (i.e., filters) in the CONV layer that are connected to a certain area of the input volume depends on the depth of the output volume. In the presence of oriented edges, blobs, or color, each filter generates an activation map that "activates."

  The number of filters we are currently learning in the current layer, or K, will determine the depth of the activation map for a specific CONV layer. The depth column is the collection of filters that are all "looking at" the same input location (x, y).
- **Stride**: A convolution operation is defined as "sliding" a tiny matrix across a large matrix, halting at each position to perform an element-wise multiplication and addition before storing the results. This explanation is comparable to a sliding window that moves across a picture from left to right and from top to bottom.

We merely made one pixel-sized step in the convolution described above. A similar idea be extended to CNNs; for each step, a new depth column is created around the local region of the picture, and each of the K filters is convolved with the region before the output is stored in a 3D volume. The stride step size S that we often employ when generating our CONV layers.

- **Zero-padding**: When applying a convolution, we must "pad" the image's boundaries to maintain the original image size; the same is true for filters inside a CNN. We can "pad" our input along the boundaries using zero-padding so that the size of our output volume matches the size of our input volume. The parameter P governs the amount of padding we use. The following formula can be used to calculate the size of the output volume $W_{out} \times H_{out} \times D_{OUT}$ [62]

$$W_{out} = \frac{W_{input} - F + 2P}{S} + 1 \quad (2.42)$$

$$H_{out} = \frac{H_{input} - F + 2P}{S} + 1 \quad (2.43)$$

$$D_{out} = K \quad (2.44)$$

With an input of size W x H x D, K is the number of (filter) kernels, spatial size F, stride S, and amount of padding P.

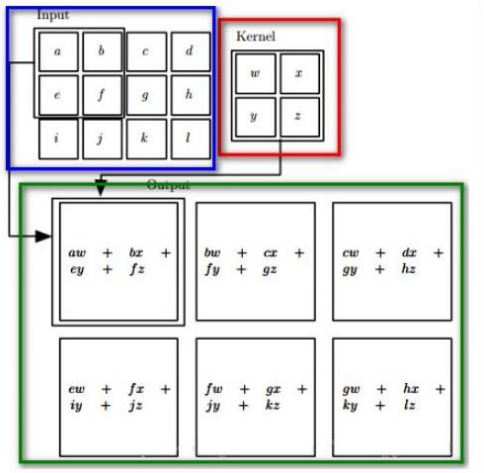

Figure (2.12) convolution process[60]

2.5.2 pooling layer

This layer is used to reduce sampling, which leads to the reduction of other layers and is similar to reducing the resolution in the field of image processing, and there are several types of them

- Max pooling
- Average pooling

Max pooling is the most common type, as it divides the image into sub-rectangles and takes only the maximum value of these sub-areas, and the most commonly used sizes are 2× 2

The output volume of size $W_{out} \times H_{out} \times D_{out}$ where:

$$W_{out} = \frac{W_{input}-F}{S} + 1 \qquad [62] \tag{2.45}$$

$$H_{out} = \frac{H_{input}-F}{S} + 1 \tag{2.46}$$

$$D_{out} = D_{input} \tag{2.47}$$

where S is stride, F is the field size (pool size)

2.5.3 Non-linearity layer (activation layer)

This layer comes directly after the convolution layer and is used to cut and determine the output generated. There are types of active functions, which are:

- Tanh
- Relu
- Leaky relu
- Sigmoid

The Relu activation layer is the most common and widely used layer, and this layer does not have weights or parameters. The input volume of the activation layer matches the output volume of the activating layer. The diagrams of activations layer shows in figure (2.13)

$$W_{output} = W_{input} \quad [62] \tag{2.48}$$

$$H_{output} = H_{input} \tag{2.49}$$

$$D_{output} = D_{input} \tag{2.50}$$

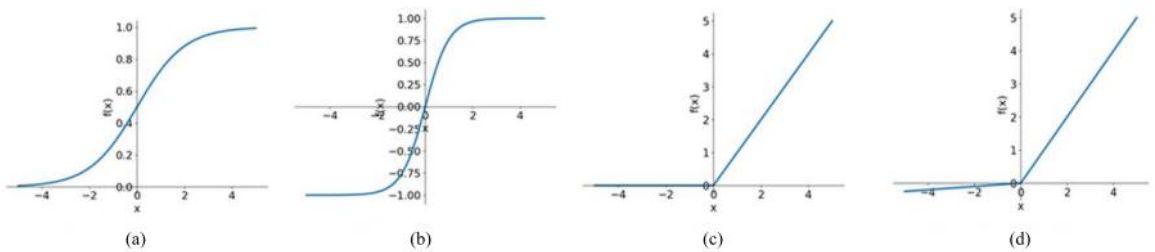

Figure(2.13) . Diagrams of (a)sigmoid, (b)tanh,(c) ReLU, (d)leaky ReLU,[63]

2.5.4 Fully connected layer(FC)

As typical for feedforward neural networks, all activations in the layer below the FC layer are fully linked to the neurons in that layer. We never apply a CONV layer, then an FC layer, then another CONV layer; instead, FC layers are always applied at the end of the network. One or two FC layers are frequently used before the soft-max classifier.

Chapter 3
The Simulation Model Description and Methodology

Chapter 3

The Simulation Model Description and Methodology

3.1 Introduction

In this study, the thesis was divided into three cases between the transmitter and the receiver. The first case is where both the transmitter and receiver were fixed. A mathematical model was designed using the Matlab program and the selection of the linear-time invariant system (LTI) system was estimated for which the frequency response was estimated using the correlation algorithm. The program was simulated after changing the controllers and choosing the highest gain value for the controller to give the least error rate. On the other hand, the transfer function of the system was changed. Noise has been added to the system by adding a block from library browser to the system , re-simulating, noticing and improving the results by changing the gain values in the controller and choosing the best value for the best frequency estimate as a table(4.7). In the second case, the transmitter is fixed and the receiver is mobile. The radar system was chosen when it was fixed and the marine target was moving with variable speed and acceleration. The target was detected and its frequency was estimated using one of the deep learning algorithms, which is the CNN. The work was compared to previous work [27] done under normal conditions in chapter four in section 4.6. The work has added clutter and noise, and good results were obtained. The signal was also classified according to speed and acceleration . In the third case the system in modern vehicles and cars. The problem was solved using the same previous algorithm CNN, and the Doppler effect was observed in both transmitter and receiver.

3.2 Simulation Model Description in frequency response estimation

In this part, the simulation describes the model for the first case when both the transmitter and the receiver are fixed. A mathematical model has been designed with the Matlab system, consisting of three main parts: the control unit, the frequency response estimator, and the system, as shown in figure (3.1). Frequency response describes the steady-state response of a system to sinusoidal inputs. Frequency estimation is when the transmitter and receiver are constant. It have designed a model in MATLAB to implement estimation process. PID controller and frequency response estimation block have been used. This block uses two modes of signal and every mode

uses a type of frequency estimation algorithm such as sine stream signal using correlation method and superposition using recursive least squares (RLS) algorithm, plant that is a close loop configuration with input of controller

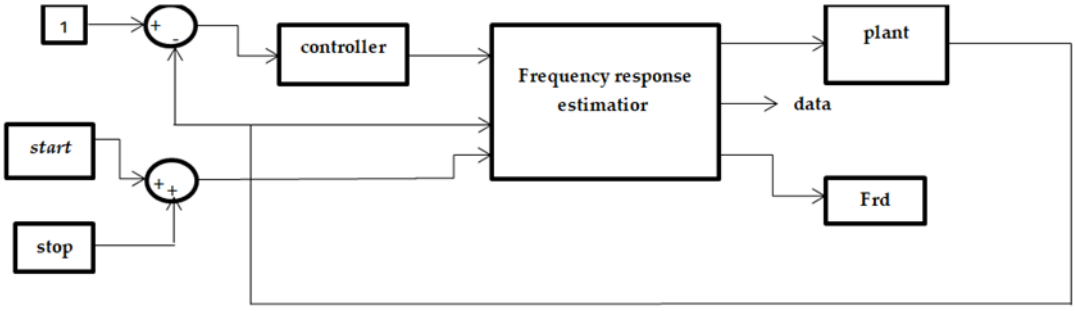

Figure (3.1) simulation model of frequency response estimation

In this thesis, we used sine stream mode in estimation for the frequency response estimator block. The simulation process as flow chart is in figure (3.2)

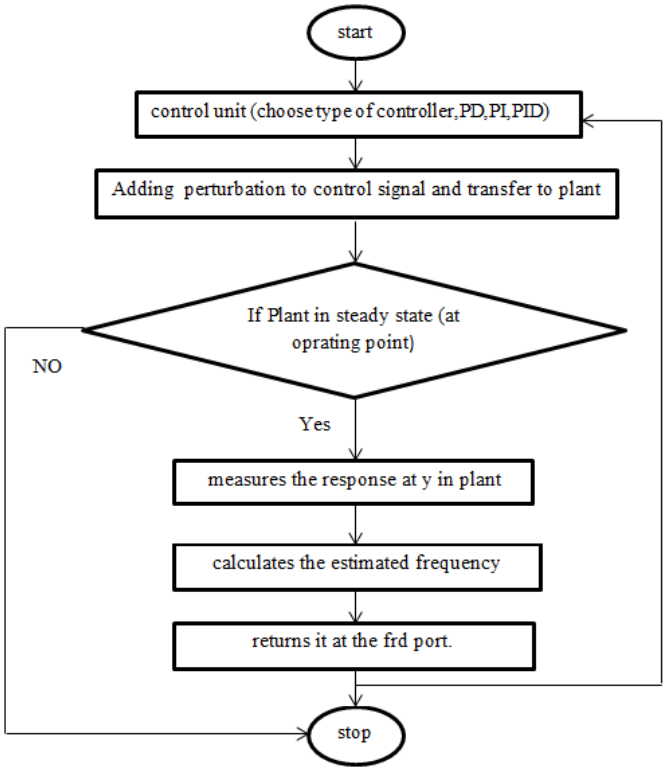

Figure (3.2) Simulink algorithm

This part of the work was carried out in two directions; The first direction is to work on the

control unit and its effect on estimating the frequency response, and the other direction is to work on changing the transmission function of the system and also note its impact on the results. The estimation process begins through the trigger in the start/stop block. Below is an explanation of each part of the model.

3.2.1 Start/stop block

This block gives a signal to start or stop the process of estimating the frequency response when preparing the signal to this block. When the signal changes from negative or (0 to 1)a positive, the estimation process begins, and when the signal changes from positive to zero or negative, the frequency estimation process ends. In this work, the amplitude value is constant for each. The frequencies and its value is 1, so when you move from zero to one, the estimation process begins, and vice versa, the estimation process ends. The Simulink length is

$$L_s = \sum_i \frac{2\pi}{w_i}\left(N_{set,i} + N_{estim,i}\right) + 2T_s N_{freq,} \quad [43] \tag{3.51}$$

$where\ L_s$ represent Simulink length

w_i represent ith frequency when the frequencies parameter in(rad/s)

$N_{freq,}$ represent number of frequencies

$N_{set,i}$ represent the value of settling priod parameter

$N_{estim,i}$ is the estimation period number

T_s is the sampling time of Simulink

3.2.2 Controller

It is the feedback control mechanism, which is widely used in industrial control systems and is considered an inverse control mechanism in the control loop. It is used to measure the error ratio between the measured process and the desired set point.

Three types of controllers were used in this model(PD,PI,PID)controller, and the gain value of each type was changed to get the least error ratio between the frequency response and the frequency response estimate.

They represent parallel form controller and figure (3.3) shows the structure of PID controller

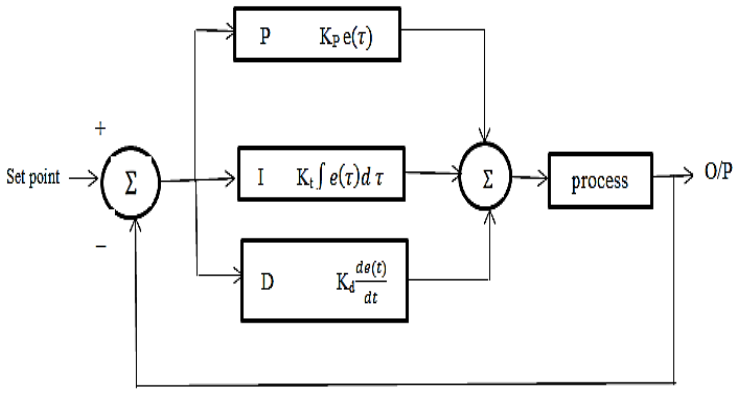

Figure (3.3) PID controller structural

It works here in parallel in this block. The type of controller is chosen. In this work, we initially chose the PID controller. The results were bad, and then we changed the gain values for the derivation part, and the best values for frequency estimation were obtained when the gain values Kp, Ki, and Kd were (5, 500, 2.5) respectively as in figure (4.2). Then the controller was changed to all its types. The best frequency estimate was obtained by changing the values of the gain. The best values of the gain were tabulated to get the best estimate as in the fourth chapter.
The work of the controller is to convert the input signal to the estimation block, which in turn adds to the disturbance signal and then transmits it to the system. When it is in a stable state, the system output is transmitted in a closed loop to the (frd block). A branch of it is to enter the modulator again to compare with another signal, and so on, since the sine stream signal enters one signal after another with the same amplitude but with a different frequency.

3.2.3 Frequency Response estimator

This block is the one concerned with the estimation process, as it contains several important parameters to complete the estimation process as figure (3.4)

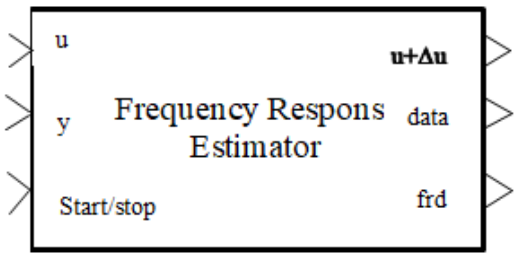

Figure (3.4) frequency response estimator block

- **start /stop port:** this port connected with start/stop block to start estimation process and end it.
- **y port:** This port is included in the system output after the estimation process in a closed loop with the system.
- **u port:** This port receives the signal from the controller and transmits it to the system.
- **u+Δu port:** At this port, the perturbation is added to the control signal during the estimation process.
- **data port:** The signal of this port contains the data collected during the simulation process, including the disturbance prepared for the system.
- **frd port:** The signal of this port contains the frequency rating response of the system for each specified frequency.

When the simulation is started, the controller signal enters the frequency response estimator block from port u to port u+Δu immediately after adding the perturbation. The system enters when it is in a stable state and operating at its nominal working point. The system outputs the simulation results to the y port, and the data is transmitted to the data port. Also, one of the characteristics of the frequency response estimator is that it shows the results in the form of a pod-plot to note the convergence of the frequency response with its estimation. Then, the comparison is made between the output and the input of the controller with another signal and extracting the error rate, thus a closed loop between the controller and the system is achieved. When the signal turns from positive to zero in the block of start and shutdown, the process of estimating the frequency in this case is transmitted directly to the system without adding any perturbation. In this case, it does not affect the behavior of the system and is an open loop.

3.2.4 Transfer Function in plant block

This part contains the system used, which is the linear time-invariant system, and contains its own transfer function, on the basis of which the frequency response is estimated. This system is without noise and consists of three parts as in figure (3.5)

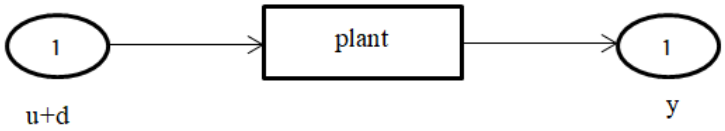

Figure (3.5) sub-system plant block (LTI system)

- **u+d port:** This port represents the input to the subsystem.
- **linear time-invariant system(LTI) block:** This block specified parameter of time invariant system such as transfer function.

  In this work, the transfer function of the system has been changed by changing (gain, zeros, and poles) ,which in turn changes the frequency response and accordingly changes the frequency response estimate for different cases. This is the absence of noise. Noise has been shed on the system by adding the Band limited white noise block to the subsystem and re-implementation of the simulation and observation. How does noise affect the frequency response?
- **y port**: This represents output port.

3.2.5 A Description the Simulation of Frequency Response estimation with addition of noise

Noise is added to the system by adding the block to the subsystem by adding it to the input and adding it to the LTI system, as in figure (3.6)

band-limited white noise block: This block generates random numbers that are normally distributed and are suitable for use in continuous or hybrid systems

To add noise to the system, a band-limited white noise block with a value of 0.01 was added to the sub-system from the library browser in Matlab, as shown in figure (3.4). In this case, the

results are good for the PID controller as shown in figure(4.7) But when the noise value is increased to (0.1)In this case, the results are some bad, as in figure (4.8). In order to improve these results, the gain value of the derivative was changed to 0.5. In this case, the results were improved, as shown in figure (4.9). In each case, the simulation is run and the frequency response estimation process is repeated.

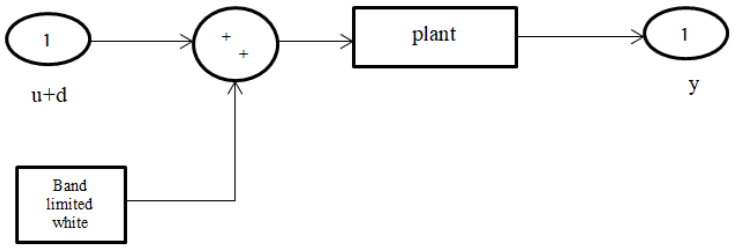

Figure (3.6)) sub-system plant block(LTI system) with noise

3.3 LFM when radar is constant and moving target

In the second case of estimating the frequency when the transmitter is stationary and the receiver is moving, We took the radar system and programmed the LFM signal received from the target when it was moving with variable speed and acceleration. In this work, the nava target was chosen as an example The following algorithm in figure (3.5) was relied on to detect the target and estimate its frequency using one of the deep learning algorithms, which is CNN.

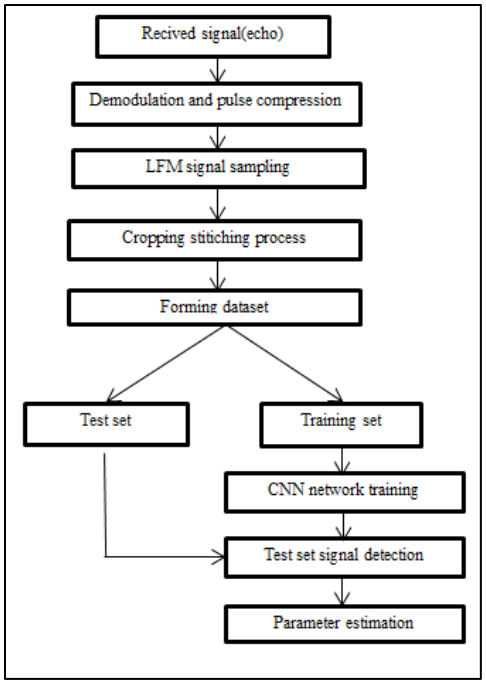

Figure (3.7) algorithm for detect LFM and parameter estimation

The radar transmits a signal in s-band of value 3GHz and 20KHz band width as equation (2.18). The radar receives a signal with a delay as well as the Doppler effect, which arises from the movement of the target at a different speed from(0 to 50) m/s and also from acceleration with a period of (0 to 5) m/s^2. The received signal is dealt with in the algorithm in figure (3.5) The algorithm is implemented by programming in m-file in Matlab.

3.3.1 Noisy signal

The situation can be studied when adding noise to the signal. Noise can be taken into account when we receive the signal from the target and the noise is Gaussian as in the equation.

$$S(t_m) = A_\circ \exp[j(2\pi f_\circ t_m + \pi\mu t_m^2)] + N(t) \quad (3.52)$$

Where $N(t)$ is represent noise

And we can compute SNR ratio to three values (0db,4db,8db),

$$\text{SNR} = \frac{\text{signal power}}{\text{noise power}} \quad (3.53)$$

$$\text{SNR}_{\text{db}} = 10\log_{10}\text{SNR}$$

3.3.2 Dataset

The data set in this thesis depends on the speed and acceleration of the target as in Table (4.12)

3.3.2.1 Single frequency signal

The signal was classified as such when the received signals from the target have a Doppler effect that is limited to the speed only. The signal is programmed according to the parameter. The speed is for an interval from (0 to 50). As for the acceleration, it is zero when the equations (2.35) related to the speed are applied. The frequency has a value, and the acceleration is zero, compensated in equation (2.36); so it is zero as shown in figure (4.14). Then, the resulting signal is converted into an image to treat the data set as images. The parameter of this signal is shown as table (3.1)

Table(3.1) parameter of single frequency signal

Parameter	**Value**
Carrier Frequency(fc)	3GHZ
Pulse width(tp)	$60\mu sec$
Band width(B)	20KHZ
Speed (m/s)	[0,50]

The dataset of single frequency signal after converted into image shown in figure (3.8)

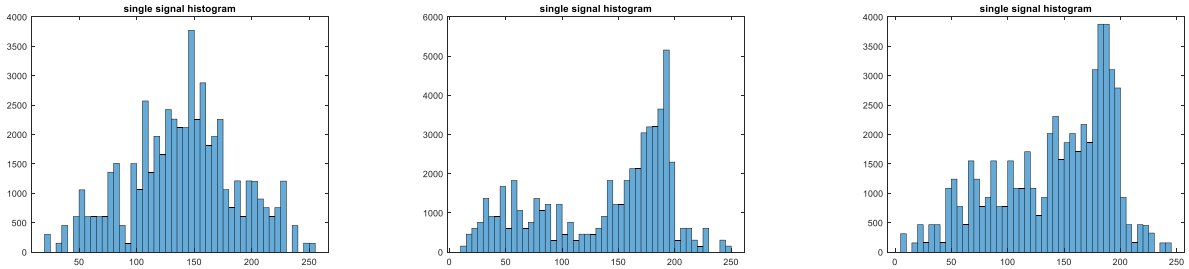

(a) (b) (c)

Figure (3.8) dataset of single frequency signal, (a)histogram with SNR=8db, (b)histogram with SNR=4db,(c)histogram with SNR=0db

This dataset represents three cases of signal –to-noise ratio (0db,4db,8db), the noise has been added to the recipient notes according to the equation (3.52).

3.3.2.2 Chirp rate signal

The signal is classified with this name when the signal received from the target is moving with acceleration only without speed and the value of acceleration is from(0 to 5) m/$s^2$and when we substitute in equation (2.39) the unified part of the equation becomes zero and the signal and howling are programmed with the value of the parameters as shown in figure (4.15), then the signal is converted into an image as figure(3.9) to be dealt with in an algorithm CNN.

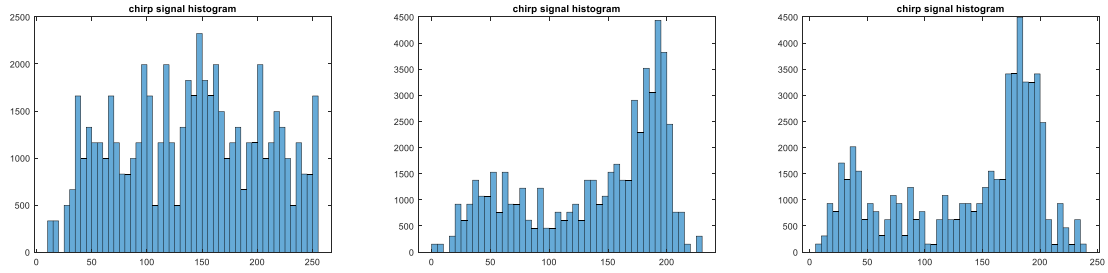

(a) (b) (c)

Figure (3.9) dataset of chirp signal, (a) histogram with SNR=8db, (b) histogram with SNR=4db, (c) histogram with SNR=0db

The image dataset represents with three cases of SNR (8db,4db,0db). The noise has been added to the receiving signal as equation (3.52).

3.3.2.3 Linear frequency modulation(LFM)signal

The received signal is classified by this name when it is received from a moving target with speed and acceleration as well, each of them in a specific period, as it moves at a speed from (0 to 50) m/s and an acceleration from (0 to 5) m/s^2as shown in figure (4.16). Compress the pulse into an image and treat it in the CNN algorithm as an image

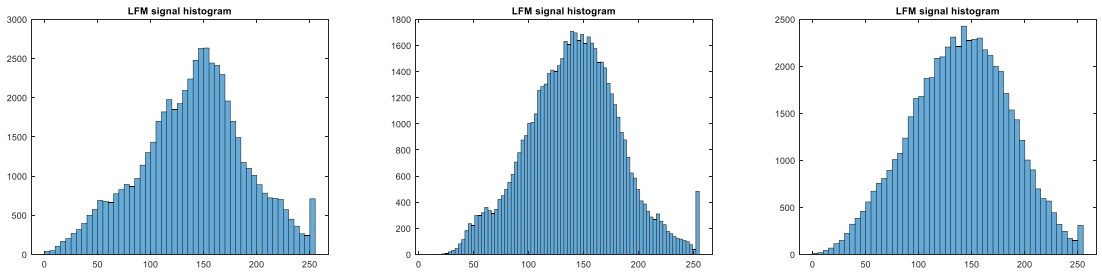

(a) (b) (c)

Figure (3.10) dataset of LFM,(a) histogram with SNR=8db,(b) histogram with SNR=4db, histogram with SNR=0db

Figure (3.8) represents image dataset of LFM with three cases of SNR (0db, 4db, 8db). The noise has been added to the receiving signal as equation (3.51)

3.3.3 Signal processing

After programming, the received signal equation (2.39) implemented demodulation and pulse compression as flow chart in figure (3.9)

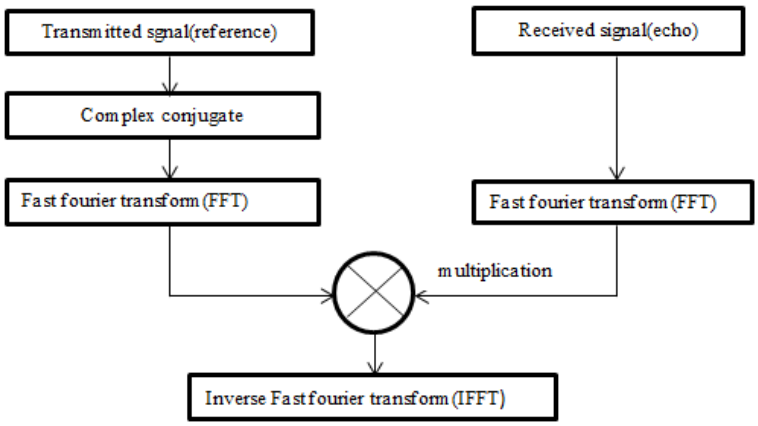

Figure (3.11) flow chart of pulse compression

A. Applying the Fourier transform to the echoes that were received (equation (2.26))
B. Taking the transmitted signal's complex conjugate (equation (2.27))
C. Performing the Fourier transform on the complex conjugated signal mentioned above.

D. Multiplication of the two FFT signals.

The pule compression signal is sampled by fs=0.8μHz. Depending on the Doppler effect, the results after this process are as explained in Chapter Four for each type of signal in the form of a single frequency signal, chirp rate signal and LFM signal.

The signal is pure and noise-free.

3.3.4 The signal received from the moving target with clutter

In the previous part, the return signal from the target was dealt with by the absence of chaos in this part. We assumed that the return signal from the moving target was in a complex environment such as clutter. In this work, we assumed the chaos was the chaos of the sea due to dealing with a moving marine target.

The signal has been programmed with Matlab and the signal has been transformed into its three types: mono-frequency, chirping signal, and linear frequency modulation signal, into images to deal with the convolutional neural network as shown in Figure(3.10)

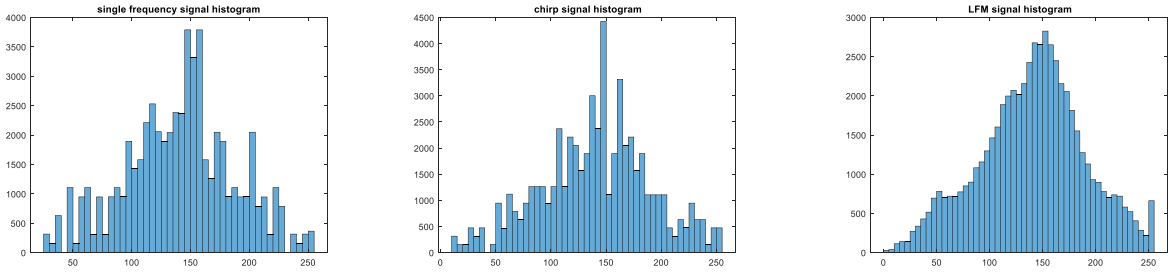

(a) (b) (c)

Figure(3.12)histogram signal with clutter where (a)single frequency histogram (b)chirp rate histogram (c)LFM histogram

3.3.5 Image Dataset

At this stage, the resulting signal, which was processed by pulse compression techniques, is converted into image by cut it into samples that form a series of one-dimensional samples. These samples are cut into pieces of equal length that form from top to bottom in the form of a two-dimensional array. This matrix can be shown in the form of an image using codes in MATLAB, and then this image is entered as a dataset for the CNN.

The images and data set were generated from the original signal categorized by speed and acceleration, so that the classes were classified according to the acceleration values that start from 0 to 5 m/s^2 and travel by 0.5, and each class generates 500 images of different speeds where an iterative loop was programmed to change the speed from 0 to 50 m/s with a shift of 0.1m . In this process, we have prepared a data set of 10 classes. Each class contains 500 images, as shown in Figure (3.13).

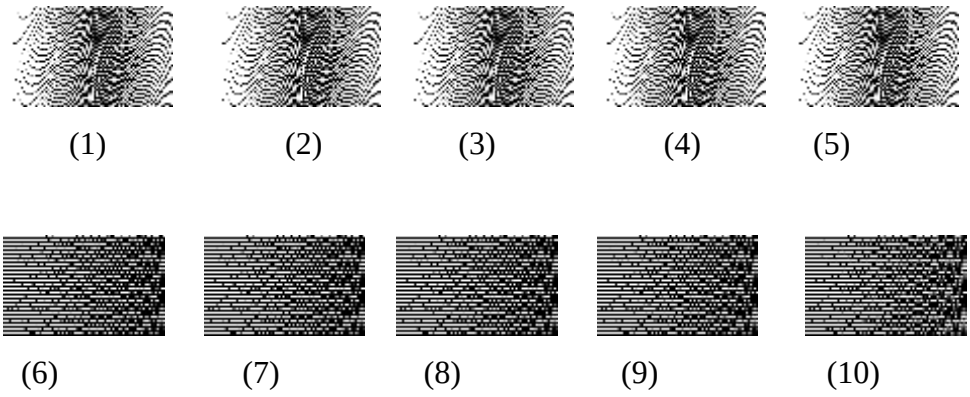

Figure (3.13) image data set in 10 classes

The figure(3.13) represents the images of the data set, where each image number represents a class, and each class represents an image of the linear frequency modulation signal that has speed and acceleration. As image number 1 represents the linear frequency signal with an acceleration of (0.5) m/s^2, and through the work of Loeb in the Matlab program, 500 images were generated from them with different speeds starting from 0.1 to 50 with the counter shifted by 0.1. Picture No. 2 is also a linear frequency inclusion signal that has an acceleration value of (1) m/s^2, and 500 images were generated from it at different speeds starting from (0.1 to 50) m/s with the counter moving by 0.1 and so on for all classes. In this case, 500 images were generated at different speeds for one acceleration value for each class. Thus, the data is prepared to enter the convolutional neural network and train the data.

3.3.6 Image processing

We have faced many difficulties in organizing the data set for the CNN. After converting the

signal into an image, the network was built using the Matlab toolbox, using the four main layers of the network as an input layer, then a convolutional layer, followed by the activation layer (Relu layer), max-pooling layer and fully connected layer. After importing the data to the network and dividing it between testing and training, and when operating the network, a bad efficiency was observed in this case. Since the work of the network depends on the strength of the data set, whenever the data set is good and strong, the efficiency of the network is good, so we concluded that there is a defect in the data set.

It has been noticed that the image values contain real and imaginary composite values, and this results from the signal processing mechanisms by means of Fourier transforms. This case was handled using the absolute code in Matlab.

We have also noted that there were negative values in the image, and since it is implemented by Relu layer in the network, its function is to cancel all negative values and make them linear values starting from zero. This means that there is a lot of information that is lost during the operation of the network and cannot be distinguished. This case was handled using the code floor as flow chart in figure (3.14), and this code shifts the values to the positive. In this way, the data set was processed to be more powerful when it enters the convolutional neural network and gives greater efficiency.as the result in chapter four

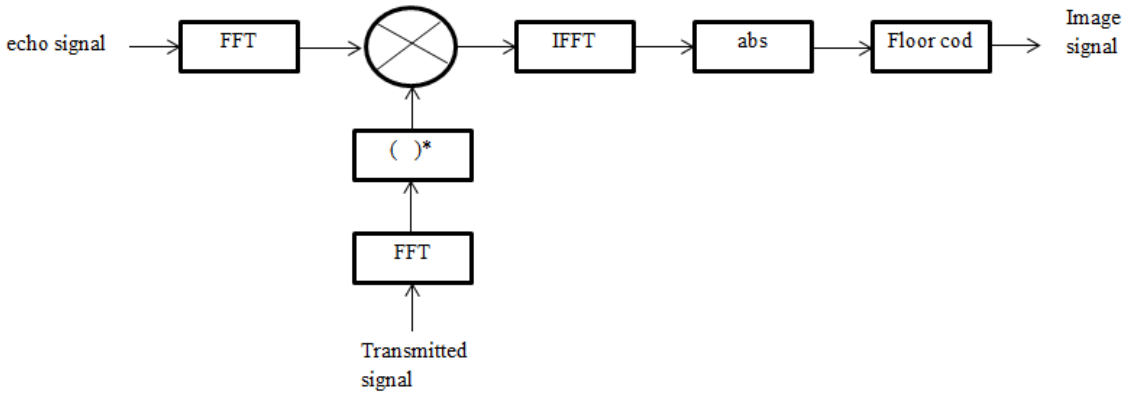

Figure (3.14) block diagram of signal processing and convert to image

The figure (3.14)shows a scheme for processing the data to be a single data set for training in

the network. The scheme starts with an echo signal to the radar and a fast Fourier transform process is performed as in Equation (2.25). As for the transmitted signal, the complex conjugate process is performed as in Equation (2.26), and then the Fourier transform is taken to the last equation as in Equation (2.27). Multiplying the two resulting signals is done. We used Equation (2.28) to get the pulse pressure signal with a frequency range. Then, the inverse Fourier Transform operation is performed as in Equation (2.29) to get the absolute value of this signal to cancel the imaginary part of it using the (abs) code. Finally, we transform the signal into a two-dimensional array to be read in the form of an image and note the values This matrix contains numbers with fractions ,which are supposed to be integers, as the image must be a positive integer from (0 to 225), so we use the code floor to remove the fractions, and the reading of the image is correct. In this case, a good image was obtained for use in the network.

3.4 Description of the Convolutional Neural Network

The convolutional neural network consists of four important basic layers, which are the convolutional layer, the non-linear active layer (relue layer), the Max Polling, and the fully Connected Layer. In this work, the network has been used as follows in figure (3.13): we used 20 hidden layer in network. And that the number of hidden layers affects the efficiency of the network in terms of extracting accurate features, and this is what distinguishes deep learning from machine learning with the presence of hidden layers.

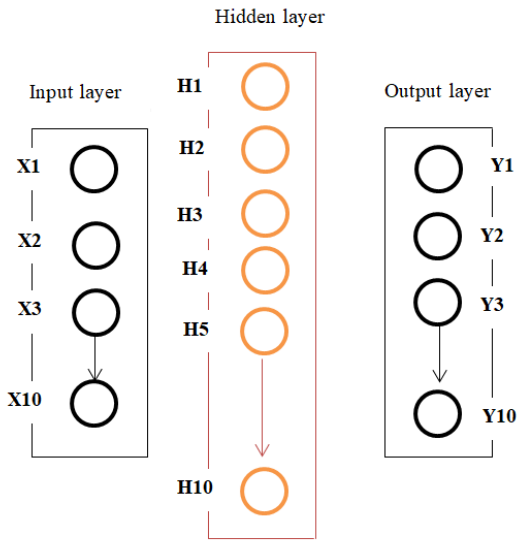

Figure (3.15) the structure of convolutional neural network used

3.5 Summary

This chapter explains the three cases discussed in the thesis ,with all the details of the work ,the algorithms adopted for each case, and the method of work until reaching the result.

Chapter 4
Simulation Setup and Results

Chapter 4

Simulation setup and results

4.1 Introduction

The results obtained are presented and discussed for the three cases in this work. The first case is the case of the sender and receiver being fixed. A mathematical model was designed using the Matlab program, and it was previously used without noise, and it was fine in this model, as the approved control was changed and the transfer function was changed. The effect of the changes observed on the frequency response and estimation for each case of change. The model also included two types of input, Sine stream or Super Possion, and for each type, an estimation algorithm, noting and discussing the results. Also, noise was added to the system and its effect on the frequency response of the system and its frequency estimation. As for the second case, when the transmitter is stationary and the target is moving, this case has been discussed using the radar system when the target is marine and moving at different speeds and accelerations, observing the effect of Doppler on the received signal and its frequency as the signal was converted into an image, displaying the results and discussing that at every particular speed we receive a signal. Only one of them differs from the other signals and represents the required frequency, as well as displaying the results of the CNN used in this case to classify the received enemy signal, each one according to its speed and acceleration.

4.2 Simulation Result in Frequency response estimation

4.2. 1 Result with change controller

In this part, we present the result of frequency response estimation in the first case on the imposition of sender and the recipient, using a model design in Matlab which contains a LTI system good in estimating the frequency where they are with a transmitter for the system, as shown in figure (4.1) below without adding any type of noise and parameter used as a table(4.1)

Table (4.1) parameter used in result (4.1)

Type of controller	PID
Proportional gain	5
Integral gain	2.5
Derivative gain	1

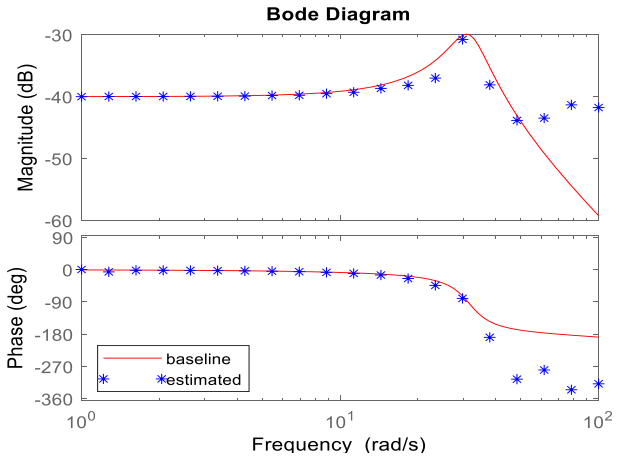

Figre (4.1) bode daigram when PID controller used with kp=5,ki=2.5,kd=1

This figure(4.1) represents the result of estimating the frequency response of a system by not adding any noise to the system, but in the presence of system perturbation and with the use of the PID type controller when the gain values kp=5,ki=2.5 and kd=1of the control parameters, we notice a large convergence between the original red line(baseline) of the frequency response and its estimate to a certain time before the completion of the estimation process. spacing between the original line of the response and the frequency estimation. This result can be improved by changing the gain value of the controller parameters to the best estimation values as in Figure (4.2) and the parameter used in simulink in ths case as table(4.2)

Table(4.2)parameter used in simulink case(4.2)

Type of controller	PID
Proportional gain	5
Integral gain	500
Derivative gain	2.5

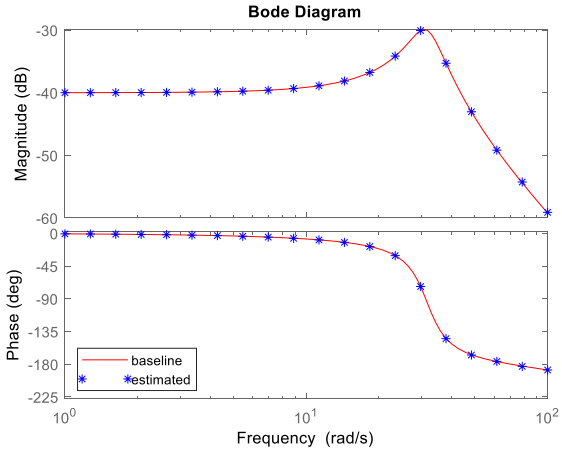

Figure(4.2) bode daigram when PIDcontroller is used ,kp=5,ki=500,kd=2.5

In Figure (4.2), the values of the controller parameters were changed to better values for the estimate, where the integration gain (ki) value was increased to 500 and the derivative gain (kd) value was increased to (2.5). We notice a significant improvement in the estimation of the frequency response of the system from the beginning of the estimation process to its end. A significant convergence was observed between the original red line of the frequency response and the points Blue, which are the values of estimating the frequency response, and the number of points represents the number of frequencies entered in the sinestream, which is 20 frequencies.

Table(4.3) simulink result for different integral gain

Ki	Simulink resut
25	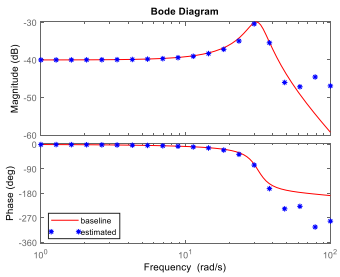

50	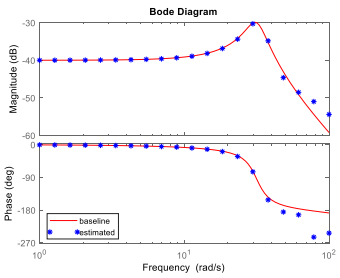
100	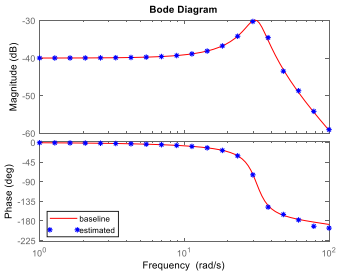
150	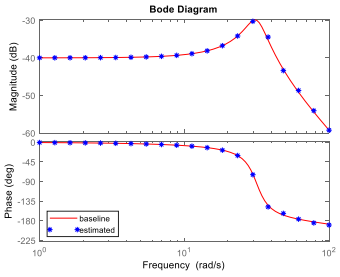
200	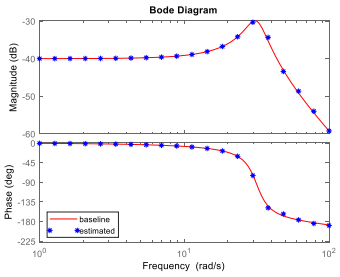
250	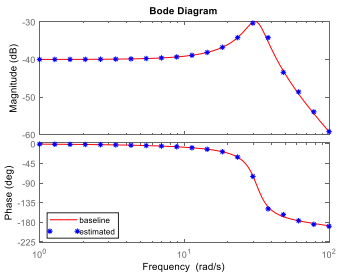

Table (4.3) represents an increase in the gain value of the integration part (Ki) we notice a change in the results for the better until we reached the lowest error rate at the value 500

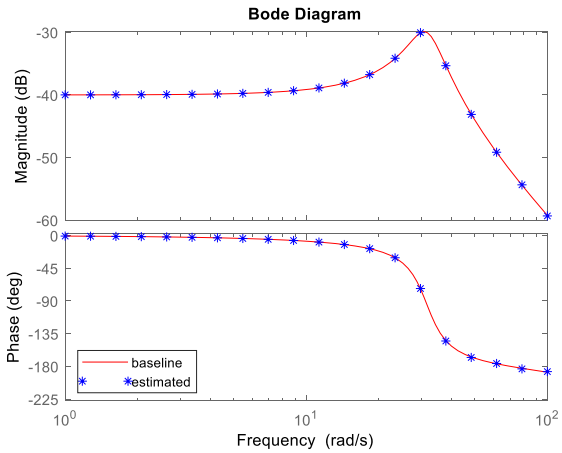

Figure(4.3) bode daigram when PD controller used with kp=5,kd=5

In Figure(4.3), another type of controller was used, the PD, and after implementing the estimation process by means of simulation, we notice that the frequency response at the beginning of the process is good, as it is noted that there is a great convergence between the frequency response, the red line, and the blue dots, which represent the estimate of the frequency response until it reaches a certain time before the process ends, a spacing occurs between the original and estimated line. This type of controller can be improved to show the best results by changing the values of the controller parameters as shown in Figure (4.4).

Table(4.4) parameter used in simulink result(4.4)

Type of controller	PD
Proportional gain	1
Derivative gain	2.5

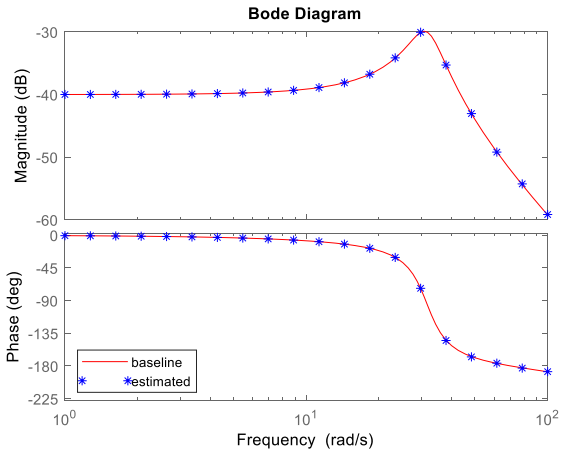

Figure (4.4) bode daigram when Pd controller used with kp=5,kd=2.5

The value of the derivative gain kd was changed to half the value of the proportional gain kp and a better estimate of the frequency response of the system was obtained.

Table (4.5)parameter used in simulink result (4.5)

Type of controller	PI
Kp	5
Ki	2.5

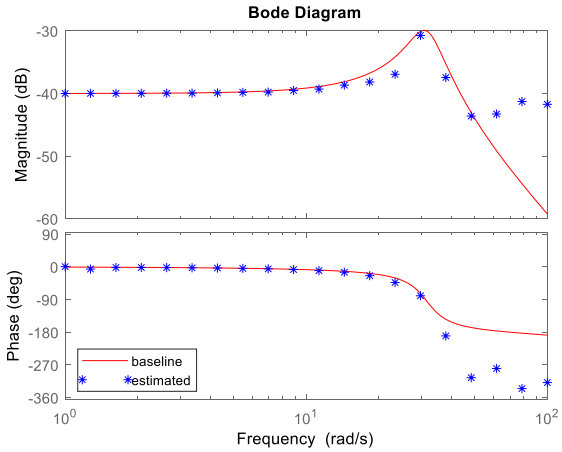

Figure (4.5) bode daigram when PI controller used with kp=5,ki=2.5

Figure(4.5) The simulation result is in the case of using the controller unite PI type values of

the proportional gain and integration are(5,2.5)respectively and the result is not good as there is spacing between the real response and estimating the response between the red line The blue stars and the result have been improved by changing the value of the integral gain from 2.5 to 500 to be the best. As a figure below

Table (4.6)parameter used in simulink result (4.6)

Type of controller	PI
Kp	500
Ki	5

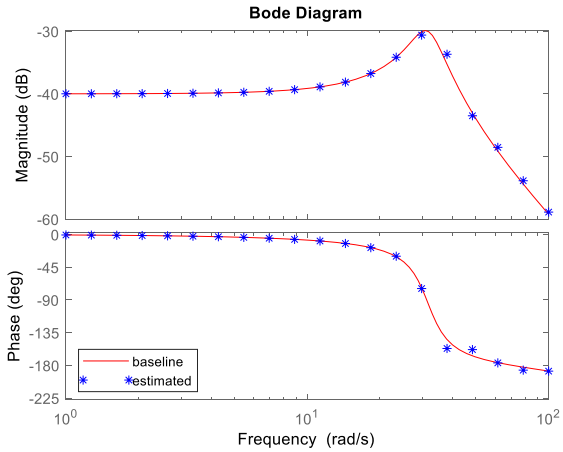

Figure(4.6) bode daigram when pI controller used with ki=500,Kp=5

In Figure (4.6) represents the frequency estimation of the system response using the PI controller with the value of the integration gain of 500.and proportional gain 0f 5 We note good results. A good convergence has been observed between the red line representing the frequency response and the blue points representing the frequency response estimation. A value can be used to gain integration. A better result than estimated was achieved. we can conclude that there are optimal values for the gaining parameters of the controller that give the best results for frequency response estimation, as shown in Table (4.7)

Tables (4.7)type of controller used with the best parameter values

type of controller	Kp	ki	Kd
PID	5	500	2.5
PI	5	500	0
PD	5	0	2.5
I	0	500	0

The mean square error (MSE) of the previous results was calculated as below equation in table

$$\text{MSE} = \frac{1}{N}\sum(\text{actual value} - \text{estimate value})^2 \quad (4.54)$$

Where N is the number of sample

Table (4.8)list of MSE for each case of controller

Type of controller	Kp	Ki	Kd	MSE
PID	5	2.5	1	0.03465
	5	500	2.5	0.0010231
PI	5	2.5	0	0.0727
	5	500	0	0.054
PD	5	0	5	0.0021
	1	0	5	0.000912
I	500	0	0	0.0726
	2	0	0	0.001022

4.2.2 Simulink Result with noise

In this section of the results, noise has been added to the system with a value of 0.01, using the PID type controller, and after simulating the model, we get the results in Figure (4.7)

Table(4.9)parameter used in simulink model with noise

Type of controller	PID
Proportional gain	5
Integral gain	2.5
Derivative gain	1
Power noise	0.01

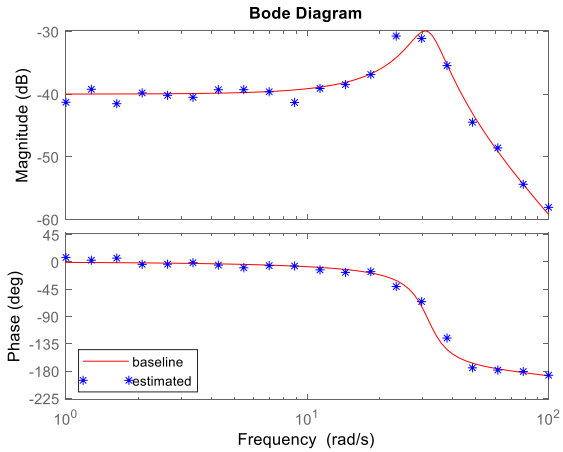

Figure(4.7) bode daigram when PIDcontroller used with adding Noise at power=0.01,kp=5,ki=500,kd=2.5

The figure(4.7) represents the best result we obtained after adding noise and using a PID typecontroller with the best values of gain at to give a good result for estimating the frequency response under white band noise at power=0.01. We also increased the noise value under more difficult conditions. After simulating the system, we note Figure (4.8)

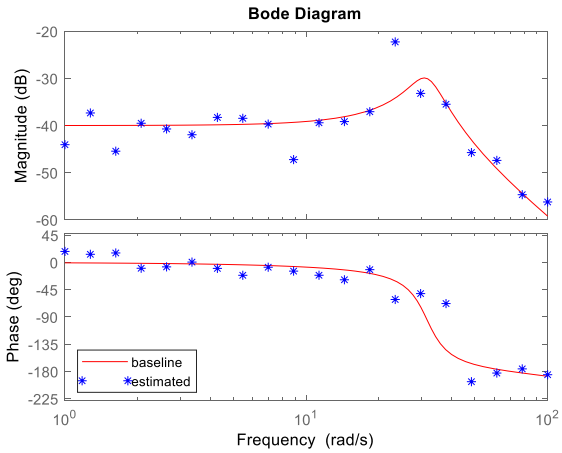

Figure(4.8) bode daigram when PID controller used with noise at power=0.1,kp=5,ki=500,kd=2.5

By increasing the noise value and using the same type of controller and the gain values for the controller parameters that were optimal in the previous case, in Figure(4.7) we notice a change in the results compared to the previous one. There is a divergence between the red line representing the frequency response and the blue points representing the frequency response estimate. The use of another type of control, which is PD

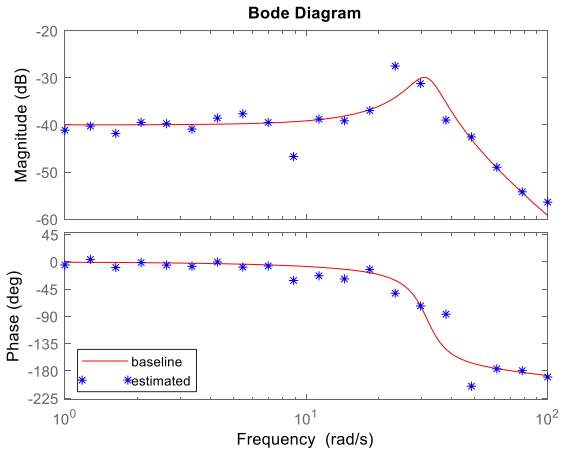

Figure(4.9) bode daigram when PD controller used with noise at power =0.1 ,kp=5,kd=0.5

Figure(4.9)is the best result for frequency response estimation that can be obtained under noise of 0.1 using the PD controller when the proportional gain values are equal to 5 and the derivative gain value is 0.5.

4.2.3 Result with change transfer function

Another part of the mathematical model has been dealt with, which is the plant block, where the transfer function is changed or both the values of poles and zeros of the system are changed to get good results in estimating the frequency response of this system, as in Figure(4.10)

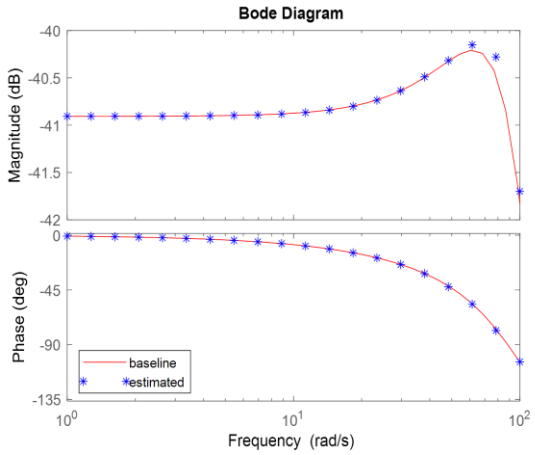

Figure (4.10) bode daigram with change the transfer function of plant with poles P1=-55+83.4i , P2=-55-83.4i,k=90,

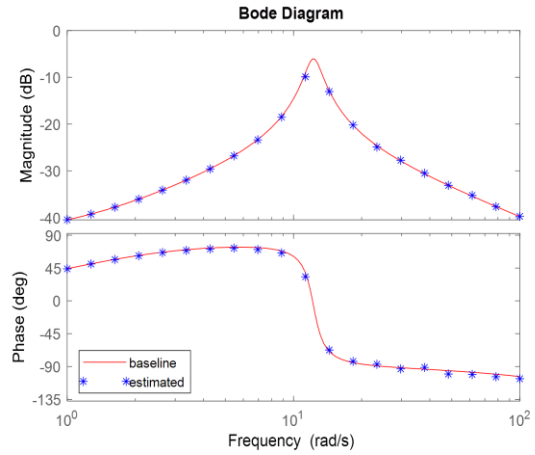

Figure (4.11) bode daigram with change the transfer function of plant with poles P1=-1+12.2i, P2=-1-12.2i,k=1,z=0

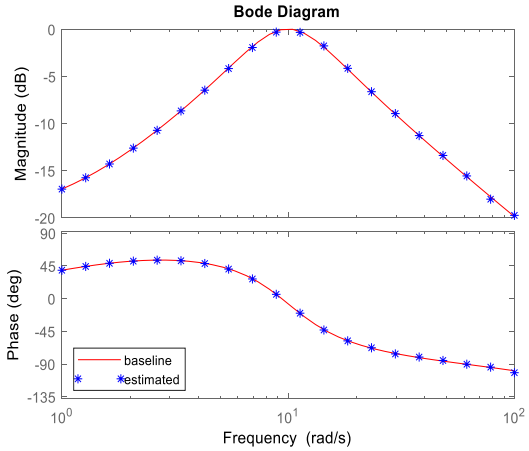

Figure(4.12) bode daigram with change the transfer function of plant with poles K=10, z=-1, P1=-5+31.22i , P2=-5-31.22i

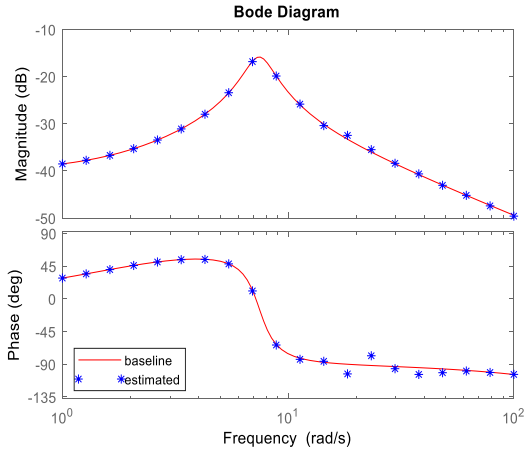

Figure(4.13) bode daigram with change the transfer function of plant with poles ,K=0.333 ,z=-1.667,P1=-1.0556+7.37i , P2=-1.0556-7.37i

The figures represent the pod-plot to estimate the frequency response to cases when the values of the transfer function of the system change. We note that Figure (4.10), Figure (4.11), and Figure(4.12) are negative, meaning the system is stable, and there are no values for zeros. We notice a fluctuation between the red line, which represents the frequency response, and the blue points, which represent an estimate. The frequency response and the results are good. As for the fourth case in Figure (4.13), there are values for negative poles in addition to a zero value. You will notice that the phase value with respect to frequency has a divergence between the

original and estimated response due to the effect of the zeros value on the system, and Table 4.2 shows the values of the different transfer function parameters used for the system.

Tables(4.10) List of various transfer function parameter values and MSE

No. of figure	**K**	**Zeros**	**Poles**	**MSE**
Figure(4.10)	90	No	P1=-55+83.4i , P2=-55-83.4i	2.5×10^{-5}
Figure(4.11)	1	0	P1=-1+12.2i , P2=-1-12.2i	8.92×10^{-6}
Figure(4.12)	10	-1	P1=-5+31.22i , P2=-5-31.22i	7.2×10^{-5}
Figure(4.13)	0.333	-1.667	P1=-1.0556+7.37i , P2=-1.0556-7.37i	4.6×10^{-3}

4.3. Simulink result of signal model in radar with moving target

Dataset used in this work in the second case depends on the movement of the target And the extent of the Doppler effect on the shape of the signal, as we assumed that the target is marine, such as a boat, for example, and that it moves at a speed ranging from(15 to 50) m/s, and that the horizontal level between the target and the radar is the received signal, as in figure (4.14)

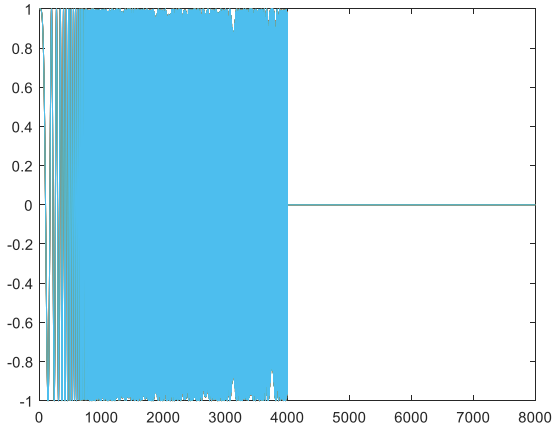

Figure (4.14) Single frequency signal ,v=50m/s,a=0

Figure (4.14) represents the signal received from the target when the boat is moving towards the

radar at a speed of 50 m/s and without rotation. It represents a single frequency signal, the amplitude is normalized and the chirping frequency is chirp up.

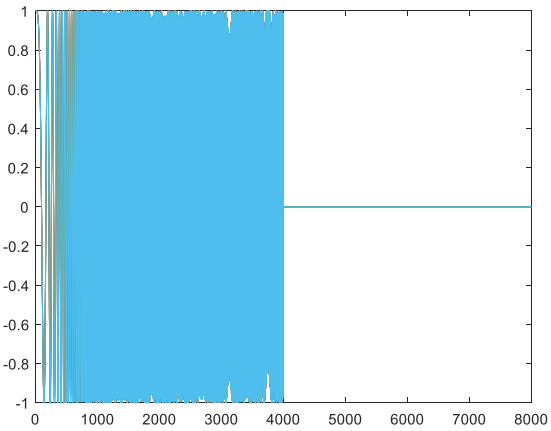

Figure (4.15) Received signal for chirp signal, v=0,a=5

Figure (4.16) represents the signal received from the target in a state of acceleration of only 5m/s^2, and the velocity is zero. In this case, the received signal is called the chirping signal.

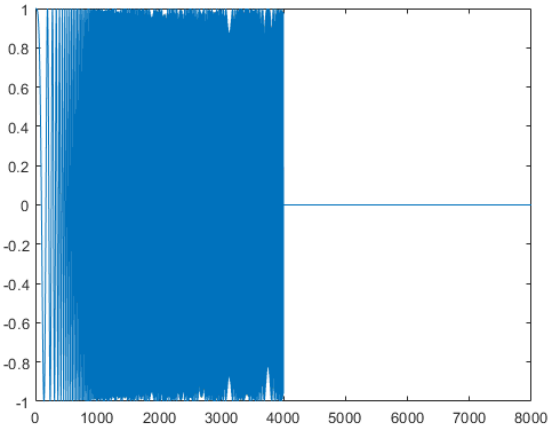

Figure (4.16) received signal for LFM, a=5,v=50

Figure (4.16) represents the signal received from the target when it is moving towards the radar at a speed of 50 m/sec and accelerating 5m/s^2. In this case, the signal is called linear frequency modulation, and the amplitude is normalized. The parameters of the received signal are in the table below

Table (4.11) Parameter used in the model

Parameter	**Value**
Carrier Frequency(fc)	3GHZ
Sampling frequency(fs)	0.8μHZ
Pulse width(tp)	60μsec
Band width(B)	20KHZ
Speed (m/s)	[0,50]
Acceleration (m/s^2)	[0,5]

Regarding the parameters of the Doppler effect on the signal received from the target, they are shown in the following table(4.9)

Table (4.12) radar signal parameter

Signal type	**Acceleration(m/s^2)**	**Velocity(m/s)**
Single frequency signal	0	[0,50]m/s
Chirp rate signal	[0-5] (m/s^2)	0
LFM signal	[0-5] (m/s^2)	[0,50]m/s

4.3.1 Simulink result of signal model with noise

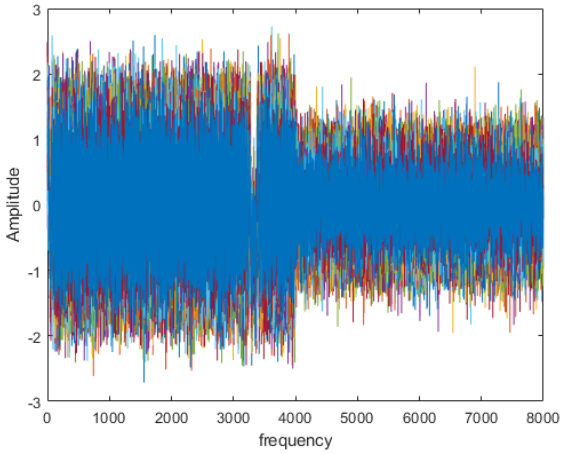

Figure (4.17) LFM with SNR=0db

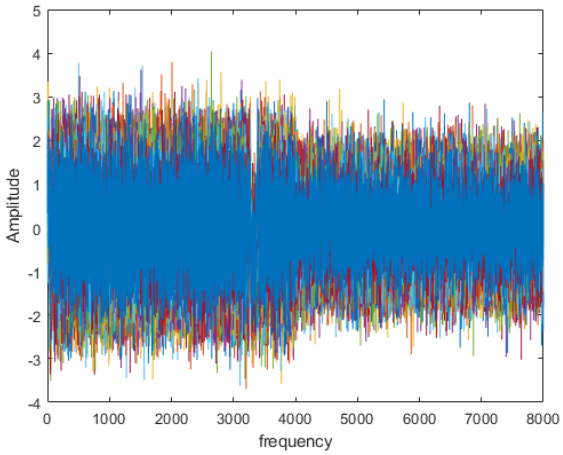

Figure (4.18) LFM with SNR=4db

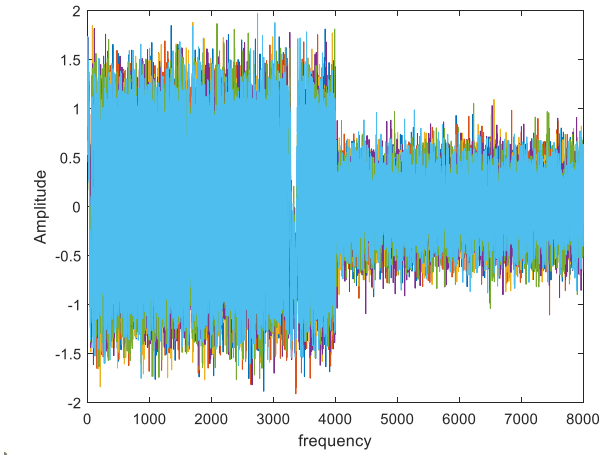

Figure (4.19) LFM with SNR=8db

The figures[(3.17), (3.18), and (3.19)] represent the signal of the linear frequency modulation signal after adding noise in three cases of the signal-to-noise ratio(SNR) of (0db, 4db, and 8db), respectively, as in Equation(3.51).

4.3.2 Simulink results of Pulse Compression

The following results represent the signal after the pulse compression process, which is noise-free and, in three cases, the signal is a single-frequency signal, a chirping signal, and a linear frequency modulation signal

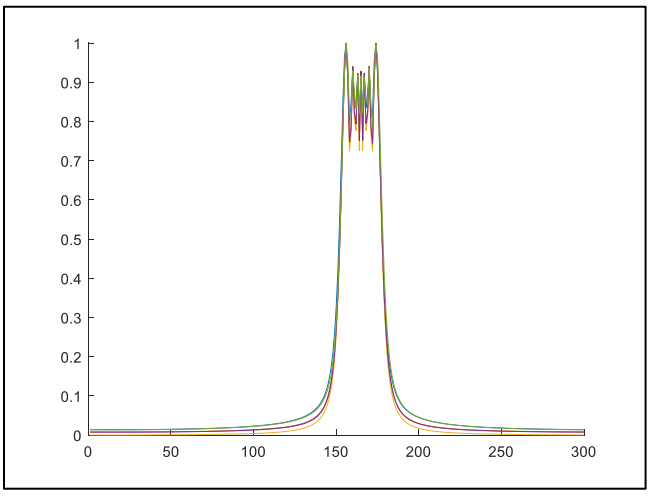

Figure (4.20) Pulse compression for single frequency signal without noise,v=1-50m/s,a=0

Figure(4.20) represents pulse compression of a single-frequency signal without noise when the velocity is from (0 to 50)m/sec, and the Doppler effect appears on the signal and the colors that cleared up in the signal resulted from the change in velocity, where we made a lobe for different values of velocity.

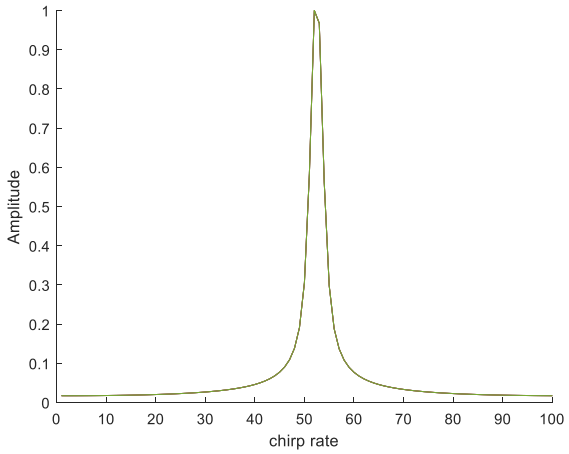

Figure (4.21) Pulse compression for chirp signal, a=5,v=0

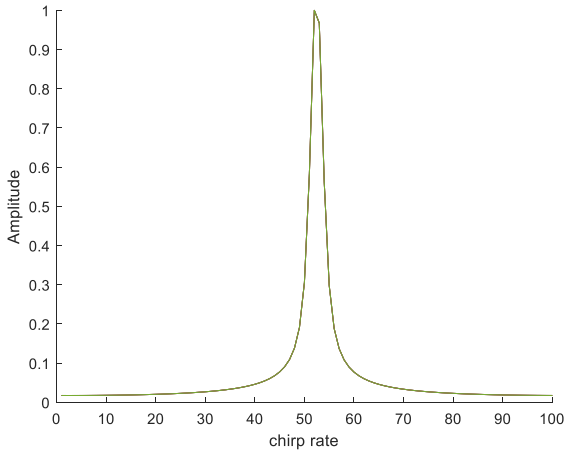

Figure (4.22) pulse compression for LFM, v=50,a=5

Figure (4.22) represents the pulse compression in the case of velocity being zero and acceleration from(0 to 5)m/s^2 and includes 419 representing the impulse pressure in the case of velocity and acceleration having a value of (0 to 50)m/s and (0 to 5) m/s^2, respectively, representing the linear frequency modulation signal as it is normalized in amplitude.

4.3.3 Simulink results of Pulse compression with noise

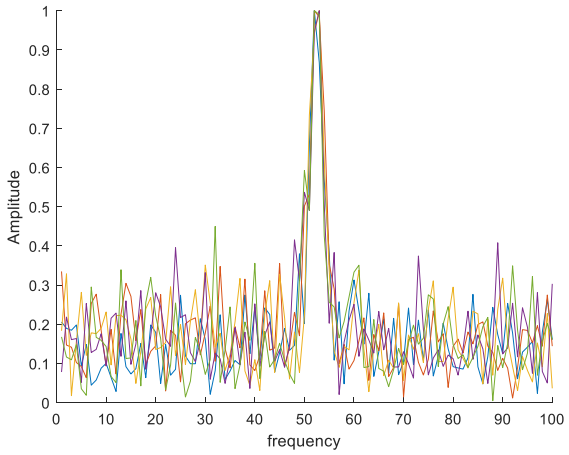

Figure (4.23) Pulse compression of LFM with SNR=0db

Figure (4.23) represents the pulse compression of the LFM signal with SNR=0db in the presence of different velocity and acceleration, and the appearance of different colors in the figure indicates the Doppler effect, which are the velocity and acceleration parameters

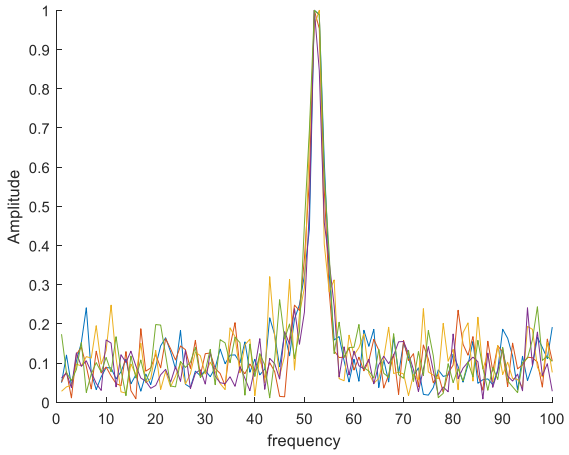

Figure (4.24) Pulse compression of LFM with 4db

Figure (4.24) represents the pulse compression of the LFM signal with SNR=4db in the presence of different velocity and acceleration, and the appearance of different colors in the figure indicates the Doppler effect, which are the velocity and acceleration parameters

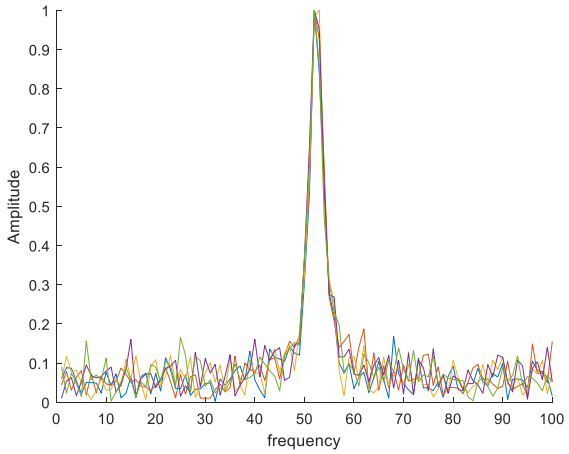

Figure (4.25) Pulse compression of LFM with SNR=8db

Figure (4.25) represents the pulse compression of the LFM signal with SNR=8db in the presence of different velocity and acceleration, and the appearance of different colors in the figure indicates the Doppler effect, which are the velocity and acceleration parameters

4.3.4 Simulation result of Convolution Neural Network result(CNN)

The set of data enters the convolutional neural network after converting the data compression signal from a one-dimensional to an eight-dimensional signal as an image to generate a set of images from it.

(a) (b) (c)

Figure (4.26) image dataset before processing (a)represent single frequency signal (b)chirp rate signal (c) LFM signal

The figure(4.26) shows the conversion of the pulse compression signal into a two-dimensional gray-level image, with the observation of the Doppler effect in classifying the signal

into a single-frequency signal, in which (a) has the effect of velocity without acceleration, and the chirping rate signal is in (b), in which the acceleration effect is without velocity, and the linear frequency modulation signal has an effect. Acceleration and acceleration are both as in(c)

Table (4.13) Parameter of CNN

The number of iterations	30
Number of hidden layer	20
The initial learning	0.01
Mini Batch Size	16
number of Epoch	5
Input size	[50,80]
Mean squared error	0.0001

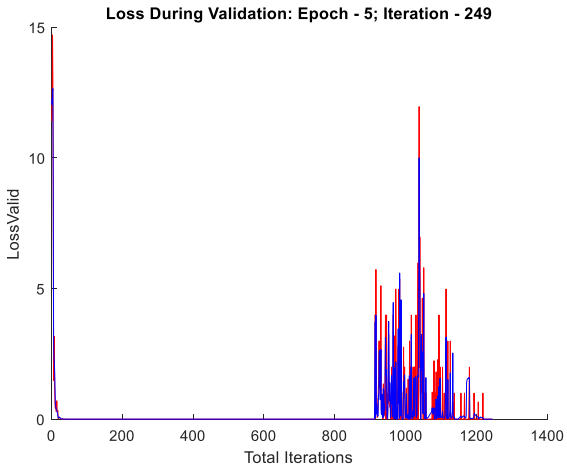

Figure (4.27) training progress

Figure (4.27) shows the process of training the data after entering the convolutional neural network, and thus we notice the mismatch of cases in many classes, which causes the network to be inefficient

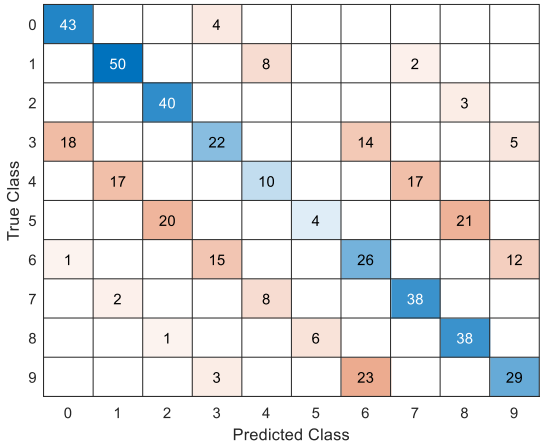

Figure (4.27) Confusion matrix represent with 10 classes classification

The figure(4.27) shows the classification output matrix that after conducting the training process for the previous data in the figure (4.26) We note that the efficiency of the network is very low and accuracy is 60%

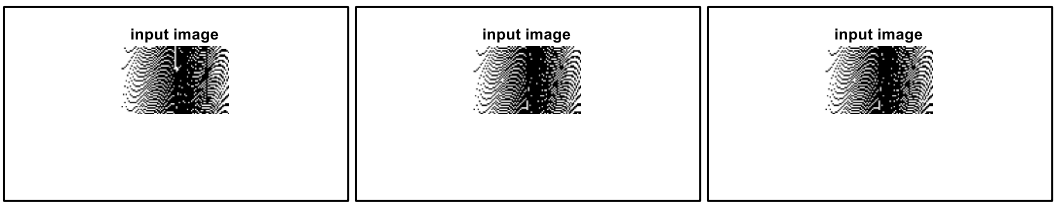

(a) (b) (c)

Figure (2.28) 2D image dataset,(a)represent single frequency signal,(b)representchirp rate signal,(c)represent LFM signal

After processing the dataset, as we mentioned in the third chapter (3.3.5), the signal was converted to a two-dimensional image of a gray level. We note that image No. (a) represents a single-frequency fence in which the effect of velocity is only for the target without acceleration, and image No.(b) represents the chirping signal in which the acceleration effect appears. For the target only without velocity, but image no (c) represents the linear frequency modulation signal in which the effect of both velocity and acceleration appears.

Each image is divided into a class containing 500 images that are generated according to the

acceleration value and speed in order to be added to the convolutional neural network algorithm.

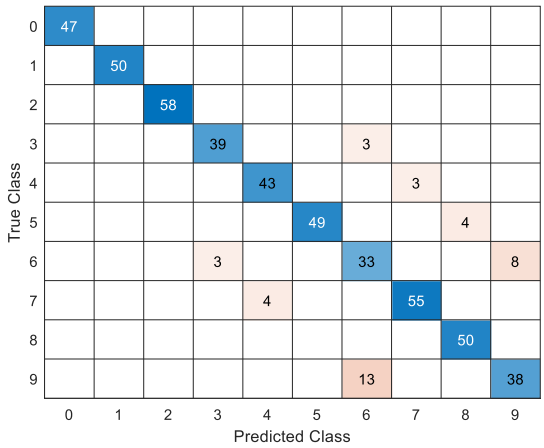

Figure (2.29) Confusion matrix after processing the dataset

Figure (2.29) shows the improvement of the network after processing the set of data entering the network, and after the training process, the accuracy increased to 92%. The network performance and accuracy can be improved by increasing the hidden layers to 30. We note that the network performance has improved to 99%.

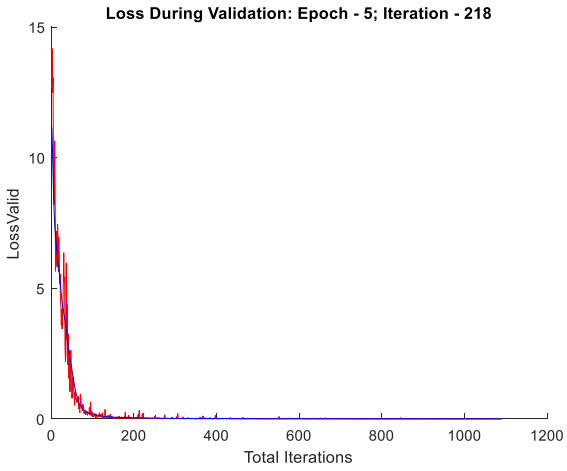

Figure (4.30) Training progress when used 30 hidden layer

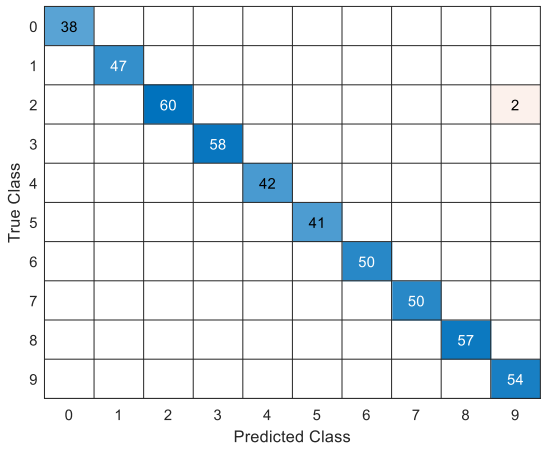

Figure (4.31) Confusion matrix after improvement

4.4 Simulink result with clutter background

This part of results represents the simulink results when the signal received from the moving target is added to a clutter signal as shown in figure(4.32)

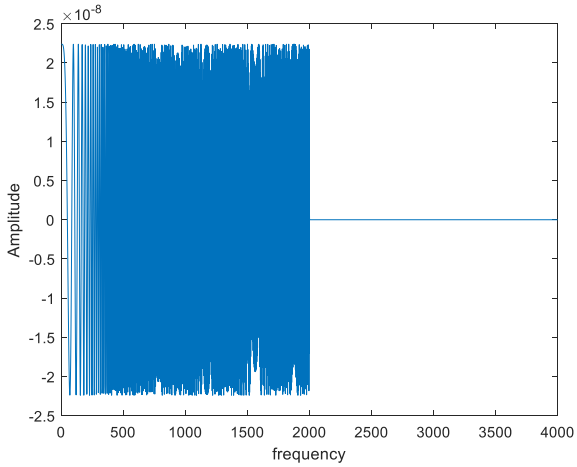

Figure(4.32)chirp signal rate

It represents the signals received from the target when its speed is zero, and the acceleration is 5m/s^2, and the type of signal represents a chirping according to the table(4.9)

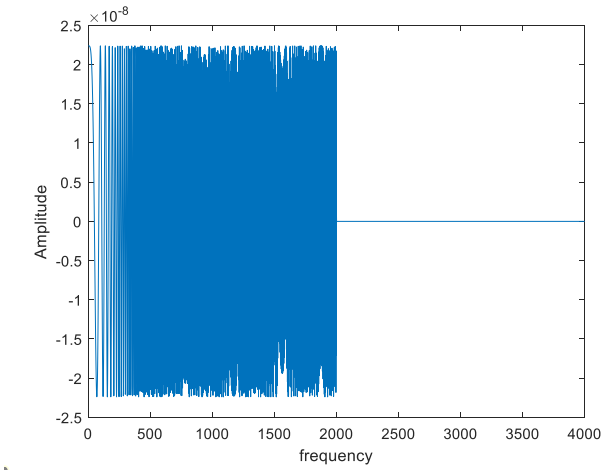

Figure(4.33)single freuency signal

The figure represents the signal received from the target when it is moving at a speed of 50 without acceleration, and it represents a single-frequency signal according to the classification of Table (4.9).

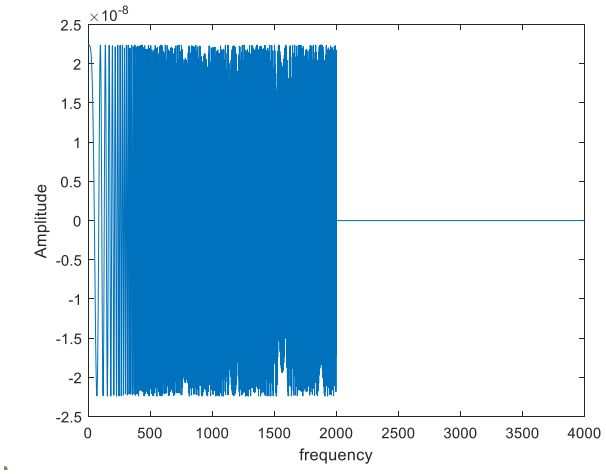

Figure(4.34)LFM signal with clutter

The figure(4.34) shows the signal received from the target moving at a speed of 50m/s and acceleration of 5m/s with the interference of an unwanted signal with it, which represents the sea clutter.We note that the amplitude of the received signal is very low due to the interference of clutter and its effect.

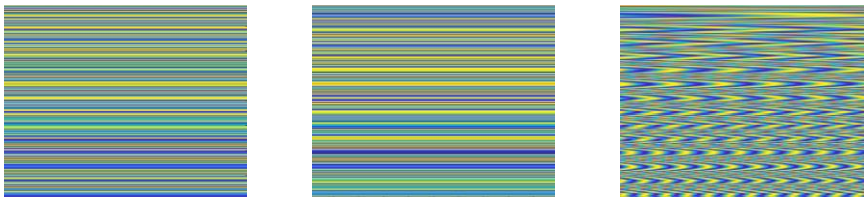

(a) (b) (c)

Figure(4.35)image signal where (a)single frequency image (b)chirp rate image (c)LFM image

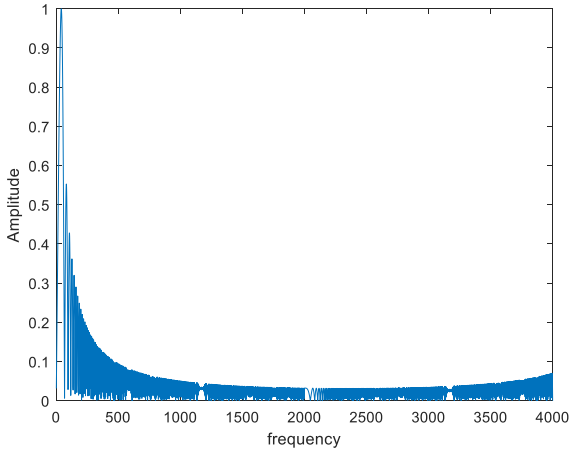

Figure(4.36)pulse compression of LFM with clutter

The figure(4.35) represents the compression of the LFM signal after processing according to the algorithm in Figure (3.5). We notice a difference in the results of the clutter-free signal represented by the displacement of the signal, while the amplitude is normalize

4.4.1 Simulink results of Convolution Neural Network with clutter

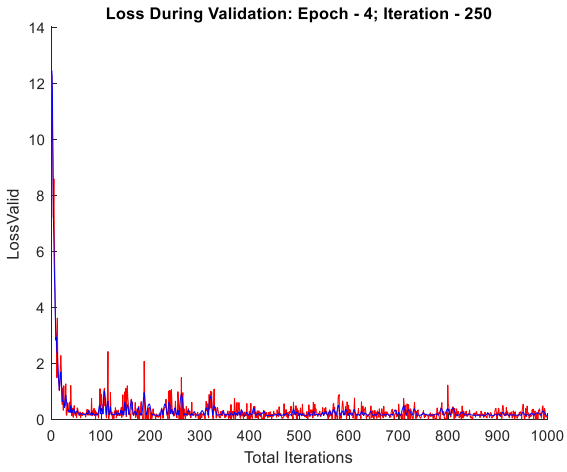

Figure (4.37) Training progress when used 30 hidden layer

The figure(4.36) represents the results of the training after adding data with clutter to the network in the form of images

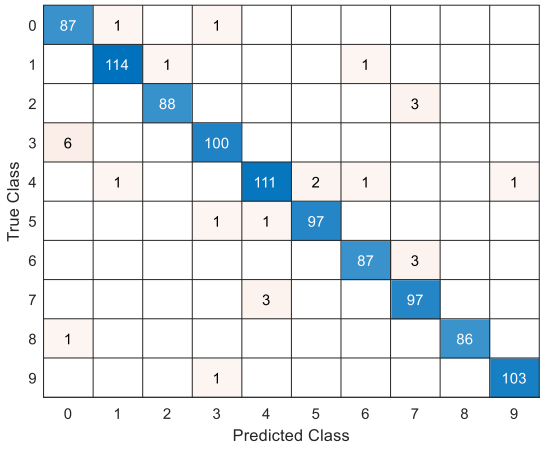

Figure(4.38) Confusion matrix

This figure represents the classification of the signal according to the speed and acceleration

when the clutter background is sea clutter and the accuracy obtained by the network is 97%.

4.5 Simulink results of signal model when both radar and target are moving

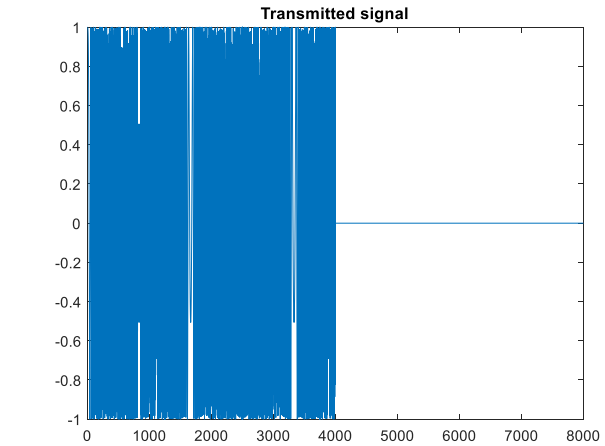

Figure(4.39)transmitted signal from radar

Figure(4.37)represent the signal sent by radar when radar is moving at speed less than the target (20m/s) and witout acceleration

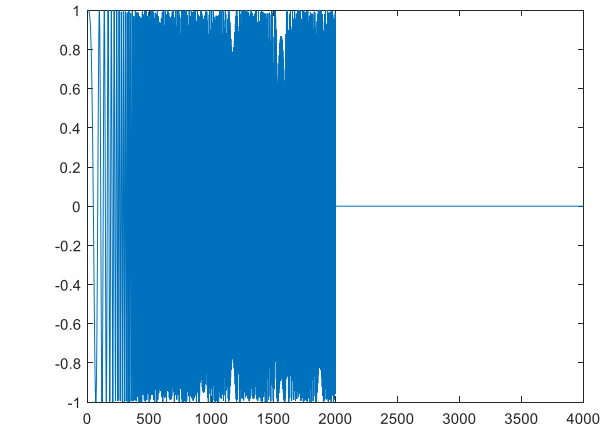

Figure(4.40) received LFM signal from target

Represents the signal received from the target when it is moving with a speed of 50m/s and acceleration of 5m/s^2

4.5.1 Simulink results of pulse compression for signal model when both radar and target are moving

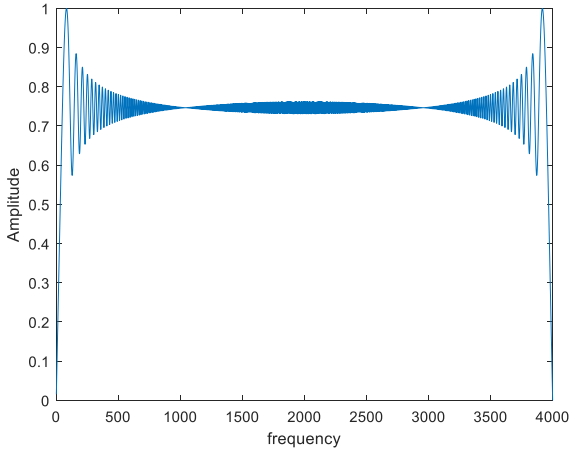

Figure(4.41)pulse compression when both radar and target are moving

The figure(4.41) represents the result of processing the signal by the pulse pressure method described in Part 4.2.4 when the radar is moving at a speed of A 20 m/s less than the target that is also moving.

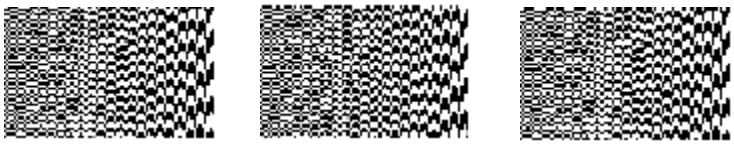

(a) **(b)** **(c)**

Figure (4.42) 2D image dataset (a)single frequency signal (b) chirp rate signal (c)LFM signal

The figure(4.42) represents the data set used in the convolutional neural network in the form of images of the signal after processing by the pulse compression technique and converting it from one-dimensional to two-dimensional for each type according to the classification of the

signal according to Table(4.12).

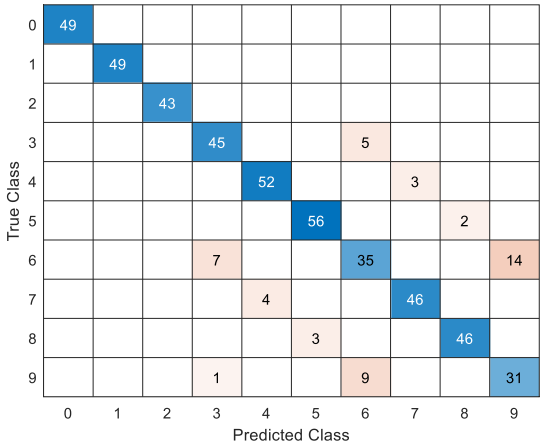

Figure(4.43) Confusion matrix

The figure(4.43) represents the result of training the data entering the convolutional neural network and classifying the received signal in the case of movement of the target and radar.where results were obtained with an accuracy of 90%.

4.6 Comparison between our work with previous work

The problem of frequency estimation was previously solved in several ways, as we mentioned in the chapter of previous studies. We dealt in this work with detecting the moving target and estimating the frequency for it using the convolutional neural network. The research was compared with the research [27] where the same algorithm was used in detecting the moving target and estimating the frequency for it but with its environment. Natural, as for our research, the target was detected and the frequency was estimated for it with a complex environment such as a clutter background.as a table(4.11)

Table(4.11) comparison between the results we have reached in our study with the results of similar studies

NO	Oure reached result	**Chen, Xiaolong;Jiang,Qiaowen Su, Ningyuan;Chen, Baoxin Guan, Jian**[27]
1	Using Fourier Transform to process the received signal	Using fractional fourier transform to process the received signal
2	Detect the target and its frequency estimation by CNN with three cases of SNR (0db,4db,8db) and get network accuracy 99%	Detect the target and its frequency estimation by CNN with two cases of SNR (0db,8db) and get network accuracy 97%
3	Target detection and frequency estimation under a complex environment,(clutter background), with a network accuracy of 97%.	Natural environment without clutter background

Chapter 5

Conclusion and Future Work

Chapter 5

Conclusion and Future Works

5.1 Conclusions

Frequency estimation is one of the very important topics due to its importance in military and security systems, which were previously treated with classical techniques.

In the first case when both transmitter and reca model was designed to estimate the frequency response of a linear time invariant system, where a change in the controller is made and the frequency response is measured. The best values of gain for different controllers are obtained as in table (4.7) to get the best estimate of the frequency response of the system. noise was added to the system. It was also found that the most usable controller is PD with the gain values of Kp and Kd as 5 and 2.5. On the other hand, the transfer function of the system was changed, and the frequency response estimate was calculated for each case, as in table (4.10).

In the second case, when the radar is fixed and the target is moving. We have dealt with the radar system because of its importance in the military and security systems. In this research, we have dealt with a marine target moving horizontally towards the radar with different speeds and accelerations as mentioned in table (4.12) The frequency estimate was calculated for it and the signal was converted into an image and dealt with The network. classified the received signal into three types according to the speed and acceleration, the single frequency signal, the chirp rate signal, and the linear frequency modulation signal (LFM). We have obtained an accuracy of up to 99 % after training the network. Also, this case was handled in complex conditions such as a clutter background, and after network training, an accuracy of 97% was obtained.

The third case is when the target and the radar are moving, so that the speed of the radar is less than the speed of the target, without acceleration But the target is moving with velocity and also accelerating, and the signal has been processed in the same way as in the second case, as well as using CNN to classify the signal. The network has achieved an accuracy of 90.

5.3 Future Works

In this section, we have proposed a number of important topics for future work that researchers can achieve in future:

1. Designing and implementation of nonlinear frequency estimation for multiple moving sources and multiple target moving in various speed and multiple frequency
2. Designing hard ware with FPGA implementation and do all the algorithm
3. Designing and implementing more than one parameter such as phase and amplitude
4. Using advance nonlearning optimization algorithm to find out the estimation of the frequency for the speedy fast target

References

[1] B. Bischl, U. Ligges, and C. Weihs, “Frequency estimation by DFT interpolation: A comparison of methods,” Technical Report,2009.

[2] Z. Sen, W. Jiulong, and Y. Dengyun, “Frequency estimation using nonlinear least squares and S-transform,” in 2010 3rd International Congress on Image and Signal Processing, vol. 1, pp. 138–142,2019.

[3] X. Liang, A. Liu, X. Pan, Q. Zhang, and F. Chen, “A new and accurate estimator with analytical expression for frequency estimation,” IEEE Commun. Lett., vol. 20, no. 1, pp. 105–108, 2015.

[4] S. Davis and I. Bucher, “A new approach to single-tone frequency estimation via linear least squares curve fitting,” *arXiv Prepr. arXiv1904.07572*, 2019.

[5] Y.-Q. Tu and Y.-L. Shen, “Phase correction autocorrelation-based frequency estimation method for sinusoidal signal,” Signal Processing, vol. 130, pp. 183–189, 2017.

[6] V. Katkovnik and Lj. Stankovic, “Instantaneous frequency estimation using the Wigner distribution with varying and data-driven window length,” IEEE Trans. signal Process., vol. 46, no. 9, pp. 2315–2325, 1998.

[7] H. K. Kwok and D. L. Jones, “Improved instantaneous frequency estimation using an adaptive short-time Fourier transform,” IEEE Trans. signal Process., vol. 48, no. 10, pp. 2964–2972, 2000.

[8] E. Sejdic, Lj. Stankovic, M. Dakovic, and J. Jiang, “Instantaneous Frequency Estimation Using the S-Transform,” IEEE Signal Process. Lett., vol. 15, pp. 309–312, 2008.

[9] A. N. Almoosawy, Z. Hussain, and F. A. Murad, “Frequency estimation of single-tone sinusoids under additive and phase noise,” 2014.

[10] J. K. Nielsen, T. L. Jensen, J. R. Jensen, M. G. Christensen, and S. H. Jensen, “Fast fundamental frequency estimation: Making a statistically efficient estimator computationally efficient,” Signal Processing, vol. 135, pp. 188–197, 2017.

[11] A. Krizhevsky, I. Sutskever, and G. E. Hinton, “Imagenet classification with deep convolutional neural networks,” Adv. Neural Inf. Process. Syst., vol. 25, 2012.

[12] H. R. Almayyali and Z. M. Hussain, “Deep learning versus spectral techniques for

frequency estimation of single tones: Reduced complexity for software-defined radio and IoT sensor communications," Sensors, vol. 21, no. 8, p. 2729, 2021.

[13] H. Milczarek, C. Leśnik, I. Djurović, and A. Kawalec, "Estimating the Instantaneous Frequency of Linear and Nonlinear Frequency Modulated Radar Signals—A Comparative Study," Sensors, vol. 21, no. 8, p. 2840, 2021.

[14] P. Bodin, "Improvements of frequency response estimation techniques," IFAC Proc. Vol., vol. 29, no. 1, pp. 4220–4225, 1996.

[15] Z. Mao and M. Todd, "Statistical modeling of frequency response function estimation for uncertainty quantification," Mech. Syst. Signal Process., vol. 38, no. 2, pp. 333–345, 2013.

[16] J. Grauer and E. Morelli, "Method for real-time frequency response and uncertainty estimation," J. Guid. Control. Dyn., vol. 37, no. 1, pp. 336–344, 2014.

[17] B. Polajžer, D. Dolinar, and J. Ritonja, "Estimation of area's frequency response characteristic during large frequency changes using local correlation," IEEE Trans. Power Syst., vol. 31, no. 4, pp. 3160–3168, 2015.

[18] F. Liu, J. Chen, and H. Qin, "Frequency response estimation of floating structures by representation of retardation functions with complex exponentials," Mar. Struct., vol. 54, pp. 144–166, 2017.

[19] O. Myronchuk, O. Shpylka, and S. Zhuk, "Algorithm of channel frequency response estimation in orthogonal frequency division multiplexing systems based on Kalman filter," IEEE 15th International Conference on Advanced Trends in Radioelectronics, Telecommunications and Computer Engineering (TCSET), pp. 31–34,2020.

[20] J. Wang, S. Su, and Z. Chen, "Parameter estimation of chirp signal under low SNR," *Sci. China Inf. Sci.*, vol. 58, no. 2, pp. 1–13, 2015.

[21] M. Joneidi, A. Zaeemzadeh, S. Rezaeifar, M. Abavisani, and N. Rahnavard, "LFM signal detection and estimation based on sparse representation," in 2015 49th Annual Conference on Information Sciences and Systems (CISS*)*, pp. 1–5,2015.

[22] Q. Chen, Y. Li, and M. Zhu, "Fast algorithm for parameter estimation of LFM signals under low SNR," in AIP Conference Proceedings, vol. 1839, no. 1, p.2017.

[23] A. Serbes, "On the estimation of LFM signal parameters: analytical formulation," IEEE Trans. Aerosp. Electron. Syst., vol. 54, no. 2, pp. 848–860, 2017.

[24] G. Bai, Y. Cheng, W. Tang, and S. Li, “Chirp rate estimation for LFM signal by multiple DPT and weighted combination,” IEEE Signal Process. Lett., vol. 26, no. 1, pp. 149–153, 2018.

[25] X. Dong, S. Chen, G. Xing, Z. Peng, W. Zhang, and G. Meng, “Doppler frequency estimation by parameterized time-frequency transform and phase compensation technique,” IEEE Sens. J., vol. 18, no. 9, pp. 3734–3744, 2018.

[26] Y. Guo and L. Yang, “Method for parameter estimation of LFM signal and its application,” *IET Signal Process.*, vol. 13, no. 5, pp. 538–543, 2019.

[27] X. Chen, Q. Jiang, N. Su, B. Chen, and J. Guan, “LFM Signal Detection and Estimation Based on Deep Convolutional Neural Network,” in *2019 Asia-Pacific Signal and Information Processing Association Annual Summit and Conference (APSIPA ASC)*, pp. 753–758,2019.

[28] X. Zhang, C. Wang, C. Yang, and Q. Lin, “Efficient moving targets chirp rate estimation method in synthetic aperture radar,” in 2019 International Radar Conference (RADAR), pp. 1–5,2019.

[29] F. Xi, Y. Xiang, Z. Zhang, S. Chen, and A. Nehorai, “Joint angle and Doppler frequency estimation for MIMO radar with one-bit sampling: A maximum likelihood-based method,*”* IEEE Trans. Aerosp. Electron. Syst., vol. 56, no. 6, pp. 4734–4748, 2020.

[30] U. Erdenebayar, H. Kim, J.-U. Park, D. Kang, and K.-J. Lee, “Automatic prediction of atrial fibrillation based on convolutional neural network using a short-term normal electrocardiogram signal,” J. Korean Med. Sci., vol. 34, no. 7, 2019.

[31] O. Abdeljaber, S. Sassi, O. Avci, S. Kiranyaz, A. A. Ibrahim, and M. Gabbouj, “Fault detection and severity identification of ball bearings by online condition monitoring,” IEEE Trans. Ind. Electron., vol. 66, no. 10, pp. 8136–8147, 2018.

[32] D. R. Bruno and F. S. Osorio, “Image classification system based on deep learning applied to the recognition of traffic signs for intelligent robotic vehicle navigation purposes,” in 2017 Latin American Robotics Symposium (LARS) and 2017 Brazilian Symposium on Robotics (SBR), pp. 1–6,2017.

[33] S. Ren, K. He, R. Girshick, and J. Sun, “Faster r-cnn: Towards real-time object detection with region proposal networks,” Adv. Neural Inf. Process. Syst., vol. 28, 2015.

[34] F. Schroff, D. Kalenichenko, and J. Philbin, “Facenet: A unified embedding for face

recognition and clustering," in Proceedings of the IEEE conference on computer vision and pattern recognition, pp. 815–823,2015.

[35] J. Huang, W. Zhou, H. Li, and W. Li, "Attention-based 3D-CNNs for large-vocabulary sign language recognition," IEEE Trans. Circuits Syst. Video Technol., vol. 29, no. 9, pp. 2822–2832, 2018.

[36] A. J. G.-C. and Francisco Pastor * , Juan M. Gandarias and J. M. Gómez-de-Gabriel, "Using 3D convolutional neural networks for tactile object recognition with robotic palpation," Sensors, vol. 19, no. 24, p. 5356, 2019.

[37] S. M. Kay, Fundamentals of statistical signal processing: estimation theory. Prentice-Hall, Inc., 1993.

[38] R. N. Bracewell and R. N. Bracewell, The Fourier transform and its applications, vol. 31999. McGraw-Hill New York, 1986.

[39] V. Shutko, L. Tereshchenko, M. Shutko, I. Silantieva, and O. Kolganova, "Application of spline-fourier transform for radar signal processing," in 2019 IEEE 15th International Conference on the Experience of Designing and Application of CAD Systems (CADSM), pp. 1–4,2019.

[40] D. Sundararajan, The discrete Fourier transform: theory, algorithms and applications. World Scientific, 2001.

[41] Z. M. Hussain, A. Z. Sadik, Digital signal processing: an introduction with MATLAB and applications. Springer Science & Business Media, 2011.

[42] C. A. Kluever, Dynamic systems: modeling, simulation, and control. John Wiley & Sons, 2020.

[43] B. Bao, J. Guo, B. Zhang, and F. Zhou, "Frequency Response Estimation Method for Modelica Model and Frequency Estimation Toolbox Implementation," in Proceedings of the 13th International Modelica Conference, Regensburg, Germany, March 4–6, 2019, 2019, no. 157.

[44] S. Lapapong, A. A. Brown, K. S. Swanson, and S. N. Brennan, "Zero-moment point determination of worst-case manoeuvres leading to vehicle wheel lift," Veh. Syst. Dyn., vol. 50, no. sup1, pp. 191–214, 2012.

[45] V. Toochinda, "Digital PID controllers," Artic. Publ. http//www. Control. com, vol. 20, 2011.

[46] K. Patel, U. Neelakantan, S. Gangele, J. G. Vacchani, and N. M. Desai, “Linear frequency modulation waveform synthesis,” in 2012 IEEE Students’ Conference on Electrical, Electronics and Computer Science, pp. 1–4,2012.

[47] R. Bassem, “Mahafza. Radar Systems Analysis and Design Using Matlab.” Chapman & Hall/CRC. Washington, DC,2000.

[48] V. J. Arya and V. Subha, “Pulse compression using linear frequency modulation technique,” in 2017 International Conference on Intelligent Computing, Instrumentation and Control Technologies (ICICICT), pp. 921–926,2017.

[49] M. Zhan *et al.*, “Space maneuvering target integration detection and parameter estimation for a spaceborne radar system with target Doppler aliasing,” IEEE J. Sel. Top. Appl. Earth Obs. Remote Sens., vol. 13, pp. 3579–3594, 2020.

[50] A. O. M. Aldow, “Target Detection and Reduction of Interrupting Signals in Coherent MIMO Radar.” Sudan University of Science and Technology, 2017.

[51] E. Markin, Principles of Modern Radar Missile Seekers. Artech House, 2022.

[52] Q. Zhang, Y. Luo, and Y. Chen, Micro-Doppler characteristics of radar targets. Elsevier, 2016.

[53] A. Eden, “The Search for Christian Doppler,” in The Search for Christian Doppler, Springer, pp. 1–4,1992.

[54] V. C. Chen, The micro-Doppler effect in radar. Artech house, 2019.

[55] G. V Weinberg, L. Bateman, and P. Hayden, “Constant false alarm rate detection in Pareto type II clutter,” Digit. Signal Process., vol. 68, pp. 192–198, 2017.

[56] G. V Weinberg, “Assessing Pareto fit to high-resolution high-grazing-angle sea clutter,” Electron. Lett., vol. 47, no. 8, p. 1, 2011.

[57] A. Mezache, Z. Terki, and F. Chebbara, “On the performance of non-coherent CFAR detectors in sea-clutter: A comparison study,” Int. J. Inf. Sci. Technol., vol. 6, no. 1, pp. 38–45, 2022.

[58] F. J. Abdu, Y. Zhang, M. Fu, Y. Li, and Z. Deng, “Application of deep learning on millimeter-wave radar signals: A review,” Sensors, vol. 21, no. 6, p. 1951, 2021.

[59] S. Albawi, T. A. Mohammed, and S. Al-Zawi, “Understanding of a convolutional neural network,” in 2017 international conference on engineering and technology (ICET), pp. 1–6,2017.

[60] S. Khan, H. Rahmani, S. A. A. Shah, and M. Bennamoun, “A guide to convolutional neural networks for computer vision,” Synth. Lect. Comput. Vis., vol. 8, no. 1, pp. 1–207, 2018.

[61] J. Gu *et al.*, “Recent advances in convolutional neural networks,” Pattern Recognit., vol. 77, pp. 354–377, 2018.

[62] U. Michelucci, *Advanced applied deep learning:* convolutional neural networks and object detection. Springer, 2019.

[63] Z. Li, F. Liu, W. Yang, S. Peng, and J. Zhou, “A survey of convolutional neural networks: analysis, applications, and prospects,” IEEE Trans. neural networks Learn. Syst., 2021.

الخلاصة

من أحدث المشاكل هي مشكلة تقدير التردد في ظل تشوه ألاشارة بسبب الضوضاء المحيطه مما يجعل من الصعب تقدير ترددها .في هذا العمل قد تم التعامل مع المشكله في ثلاثه حالات للتنقل بين المرسل والمستلم .
الحاله الاولى :هي حالة المرسل والمستلم ثابتين تم تصميم نموذج رياضي باستخدام برنامج الماتلاب وتقدير استجابه التردد لنظام خطي ثابت الوقت عندما يكون الادخال اشارة جيبيه وطريقه الارتباط هي الخوارزميه المستخدمه في هذه الحاله حيث تم العمل على وحدة التحكم في الموديل حيث تم استخدام كل انواع وحدات التحكم واستنتجنا ان افضل قيم الكسب للحصول على افضل استجابه تقدير تردد هي (Kp,Ki,Kd) (5,500,2.5)على التوالي وبعد تسليط الضوضاء على النظام وجدنا ان افضل وحدة تحكم لافضل تقدير لاستجابه التردد وحدة التحكم PDعندما تكون قيم الكسب Kp,Kd هي 5و2.5 على التوالي .
اما الحاله الثانيه عندمه يكون المرسل ثابت والمستلم متحرك مثل نظام الرادار والهدف يتحرك بسرعه وتعجيل مختلفين حيث يتم الكشف عن الهدف ومعالجه الاشارة باستخدام تقنيه ضغط النبضه وملاحظه تأثير دوبلر على الاشارة وتقدير تردد الاشارة المستقبلة في ثلاث حالات من نسبه الاشاره الى الضوضاء وهي (0db,4db,8db) بعد تحويلها من اشارة احادية البعد الى ثنائيه البعد والتعامل معها كصور ولقد تم استخدام خوارزمية الشبكة العصبيه التلافيفيه وهوة يعتبر مقدر غير خطي لتقدير التردد والحصول على نتائج جيده جدا وبدقه 99% ضمن ظروف البيئه الطبيعيه ايضا قد تم الكشف عن الهدف وتقدير التردد له في ظروف بيئه معقده مثل خلفية الفوضى تمت اعادة محاكاة البرنامج باستخدام CNN والحصول على نتائج بدقه 97%.
الحاله الثالثه عندما يكون كل من الهدف والرادار متحركين الرادار يتحرك بسرعه 20م/ثا والهدف يتحرك بسرعه 50م/ثا وبتعجيل 5م/ثا باستخدام نفس الشبكه CNNوتصنيف الاشارة المستلمه حسب السرعه والتعجيل الى اشارة احادية التردد واشارة الغرد واشارة التضمين الخطي والحصول على دقه تقدر ب 90%.

جمهورية العراق

وزارة التعليم العالي والبحث العلمي

جامعة الفرات الاوسط التقنية

الكلية التقنية الهندسية – نجف

الشبكات العصبيه التلافيفيه على أساس مقدر التردد غير الخطي

رسالة مـقدمة الى

قسم هندسة تقنيات الاتصالات

كجزء من متطلبات نيل درجة ماجستيرتقني في هندسة الاتصالات

من

رنا حسن جعفر

بكالوريوس هندسة تقنيات الاتصالات

اشراف

ألاستاذ الدكتور احمد طه عبد السادة الجياشي

2022/